RESEARCH ARTICLE

WILEY

miR-193b represses influenza A virus infection by inhibiting Wnt/β-catenin signalling

Xiaoyun Yang[1,2] | Chunling Zhao[2] | Gayan Bamunuarachchi[1,2] | Yang Wang[2] | Yurong Liang[1,2] | Chaoqun Huang[1,2] | Zhengyu Zhu[1,2] | Dao Xu[1,2] | Kong Lin[1,2] | Lakmini Kumari Senavirathna[1,2] | Lan Xu[2] | Lin Liu[1,2] [ID]

[1] Oklahoma Center for Respiratory and Infectious Diseases, Oklahoma State University, Stillwater, Oklahoma, USA

[2] Lundberg-Kienlen Lung Biology and Toxicology Laboratory, Department of Physiological Sciences, Oklahoma State University, Stillwater, Oklahoma, USA

Correspondence
Lin Liu, Ph.D., Department of Physiological Sciences, Oklahoma State University, 264 McElroy Hall, Stillwater, OK 74078, USA.
Email: lin.liu@okstate.edu

Funding information
National Institutes of Health, Grant/Award Numbers: AI121591, GM103648, HL116876 and HL135152; Oklahoma Center for Adult Stem Cell Research; Lundberg-Kienlen Endowment fund

Abstract

Due to an increasing emergence of new and drug-resistant strains of the influenza A virus (IAV), developing novel measures to combat influenza is necessary. We have previously shown that inhibiting Wnt/β-catenin pathway reduces IAV infection. In this study, we aimed to identify antiviral human microRNAs (miRNAs) that target the Wnt/β-catenin signalling pathway. Using a miRNA expression library, we identified 85 miRNAs that up-regulated and 20 miRNAs that down-regulated the Wnt/β-catenin signalling pathway. Fifteen miRNAs were validated to up-regulate and five miRNAs to down-regulate the pathway. Overexpression of four selected miRNAs (miR-193b, miR-548f-1, miR-1-1, and miR-509-1) that down-regulated the Wnt/β-catenin signalling pathway reduced viral mRNA, protein levels in A/PR/8/34-infected HEK293 cells, and progeny virus production. Overexpression of miR-193b in lung epithelial A549 cells also resulted in decreases of A/PR/8/34 infection. Furthermore, miR-193b inhibited the replication of various strains, including H1N1 (A/PR/8/34, A/WSN/33, A/Oklahoma/3052/09) and H3N2 (A/Oklahoma/309/2006), as determined by a viral reporter luciferase assay. Further studies revealed that β-catenin was a target of miR-193b, and β-catenin rescued miR-193b-mediated suppression of IAV infection. miR-193b induced G0/G1 cell cycle arrest and delayed vRNP nuclear import. Finally, adenovirus-mediated gene transfer of miR-193b to the lung reduced viral load in mice challenged by a sublethal dose of A/PR/8/34. Collectively, our findings suggest that miR-193b represses IAV infection by inhibiting Wnt/β-catenin signalling.

KEYWORDS

cell cycle arrest, influenza A virus, microRNA, miR-193b, vRNP nuclear import, Wnt/β-catenin signaling

1 | INTRODUCTION

Influenza A virus (IAV) infection causes annual epidemics and recurring pandemics, leading to substantial morbidity and mortality, as well as significant economic losses. IAV belongs to the family *Orthomyxoviridae* and has a segmented, negative-sense, and single-stranded RNA genome. Although vaccines remain a major means of prevention, a significant amount of time is required to develop and produce an effective vaccine against a new virus strain (Soema, Kompier, Amorij, & Kersten, 2015). Furthermore, vaccines need to be reformulated annually due to the frequent emergence of new viruses (Houser & Subbarao, 2015). Antiviral drugs, on the other hand, are essential for treatment and prophylaxis. However, the error-prone nature of the influenza RNA polymerase, due to its lack of proofreading-repair activity, makes the virus highly susceptible to mutation, resulting in its resistance to antivirals (Watanabe et al.,

2014). For example, there has been rapid emergence of IAV strains that are resistant to amantadine and rimantadine, and these antivirals are thus no longer recommended for anti-influenza treatment (Barr et al., 2007; Bright et al., 2005). Resistance against neuraminidase inhibitors, such as oseltamivir and zanamivir as well as newly developed peramivir and laninamivir, has also been reported (Barrett & McKimm-Breschkin, 2014; Hurt et al., 2009; Kamali & Holodniy, 2013; Orozovic, Orozovic, Jarhult, & Olsen, 2014). Therefore, it is increasingly urgent to develop drugs that target host factors rather than viral proteins, which is less likely to cause drug resistance.

The small coding capacity of IAV requires it to utilise the host cell machinery for its life cycle (Watanabe, Watanabe, & Kawaoka, 2010; York, Hutchinson, & Fodor, 2014). Many host proteins and signalling pathways regulate IAV infection at different stages. Early in 2003, Wurzer et al. (2003) discovered that efficient IAV propagation depends on the activation of host caspase-3, a central player in apoptosis, as the presence of a caspase-3 inhibitor in cells strongly impairs viral replication. Several studies have shown that IAV stabilises the p53 protein, activates p53 signalling and consequently induces apoptosis in host cells (Nailwal, Sharma, Mayank, & Lal, 2015; Turpin et al., 2005; Zhirnov & Klenk, 2007). Recently, cyclophilin A was found to interact with the IAV M1 protein and thus to impair early viral replication (X. Liu et al., 2012). IAV also interacts with many other cellular pathways, including the NF-κB, PI3K/Akt, MAPK, PKC/PKR, and TLR/RIG-I signalling cascades, to overcome host defences against the virus (Gaur, Munjhal, & Lal, 2011; Ludwig & Planz, 2008; C. Zhang et al., 2014).

MicroRNAs (miRNAs) are ~22-nt small noncoding RNAs that posttranscriptionally regulate gene expression by binding the 3′-untranslated region (3′-UTR) of a target mRNA to inhibit protein translation or degrade mRNA (Y. Wang, Stricker, Gou, & Liu, 2007). Several thousand miRNAs have been identified in plants, animals, and viral genomes (Akhtar, Micolucci, Islam, Olivieri, & Procopio, 2016). miRNAs are key modulators in diverse signalling pathways (Zamore & Haley, 2005). Increasing evidence indicates that miRNAs also participate in host–virus interactions and play a pivotal role in the regulation of viral replication. For example, miR-122, a liver-specific miRNA, facilitates viral replication by targeting the 5′-UTR of hepatitis C virus RNA (Thibault et al., 2015). Cellular miR-24 and miR-93 target the viral large protein (L protein) and phosphoprotein (P protein) genes of vesicular stomatitis virus (Otsuka et al., 2007). In addition, miR-323, miR-491, and miR-654 inhibit replication of H1N1 IAV by binding the PB1 gene (Song, Liu, Gao, Jiang, & Huang, 2010). miRNA can also modulate the type I interferon (IFN) system to combat viral infection. Wang et al. has demonstrated that IFN-induced miR-155 positively regulates the host antiviral innate immune response via type I IFN signalling by targeting suppressor of cytokine signalling 1 (SOCS1; P. Wang et al., 2010).

We have recently demonstrated a beneficial role of Wnt/β-catenin signalling in IAV infection. The activation of Wnt/β-catenin with Wnt3a enhances influenza virus replication, whereas the inhibition of the pathway with iCRT14 decreases influenza infection (More et al., 2018). In the present study, we sought to identify miRNAs that regulate IAV replication by modulating the Wnt/β-catenin pathway. Here, we report the systematic screening of a miRNA expression library and identification of 20 miRNAs that modulate the activity of the Wnt/β-catenin pathway. Four selected miRNAs that inhibit the pathway, miR-193b, miR-548f-1, miR-1-1, and miR-509-1, were found to have anti-IAV activities. miR-193b suppressed IAV replication by targeting β-catenin.

2 | RESULTS

2.1 | Screening of miRNAs that alter Wnt/β-catenin signalling activity

The Wnt/β-catenin signalling pathway plays an important role in various biological processes. Several studies have shown that a number of miRNAs modulate the activity of Wnt/β-catenin signalling by regulating the expression of the pathway-related components (Anton, Chatterjee, Simundza, Cowin, & Dasgupta, 2011; T. Hu et al., 2016; K. Huang et al., 2010). To systematically identify miRNAs that regulate Wnt/β-catenin signalling, we constructed a miRNA expression library composed of 738 human miRNA precursor expression vectors and performed screening using a TOPflash reporter luciferase assay as a readout for Wnt/β-catenin signalling activity (Figure 1a). The TOPflash reporter vector contains three copies of T-cell factor (TCF)/lymphoid enhancer-binding factor (LEF) binding sites upstream of the luciferase reporter gene. The initial screening was performed in 96-well plates with three replicates. Human HEK293T cells were transfected with a TOPflash luciferase reporter plasmid, miRNA expression plasmid, and the normalisation vector, pRL-TK vector, for 24 hr and were then stimulated with Wnt3a for 24 hr, followed by the dual luciferase assay. Among 738 miRNAs, 85 miRNAs were found to up-regulate and 20 to down-regulate luciferase activity with a fold change ≥2, resulting in a hit rate of 14.2% (Figure 1a and Table S1).

To further validate the primary screen data, we repeated the reporter assay with a FOPflash vector containing mutated TCF binding sites as a negative control for TOPflash activity. If a miRNA changed the FOPflash activity similar to the TOPflash activity, the miRNA was considered to be a false positive. We selected approximately equal numbers of up- and down-regulating miRNAs (up, 24 miRNAs with a greater than or equal to threefold change, and down, 20 miRNAs with a ≥2-fold change, Figure 1b). Among the 20 down-regulating miRNAs, miR-548f-1, 548f-2, and 548f-4 have an identical mature miRNA, and thus, miR-548f-2 and 548f-4 were excluded. TOPFlash and FOPlash firefly luciferase activities, normalised to pRL-TK Renilla luciferase activity, are shown in Figure 1c for the up-regulating miRNAs and Figure 1d for down-regulating miRNAs. A ratio of normalised TOPflash/normalised FOPflash are presented in Figure 1e,f. Using a TOPflash/FOPflash ratio of 1.5 as a cut-off value, we identified 15 and five miRNAs that up- and down-regulated the Wnt/β-catenin signalling pathway, respectively.

2.2 | Identification of miRNAs with anti-IAV activities

We then tested whether the above-identified miRNAs that down-regulated the Wnt/β-catenin pathway could inhibit IAV infection. Among the five miRNAs (miR-193a, miR-193b, miR-548f-1, miR-1-1,
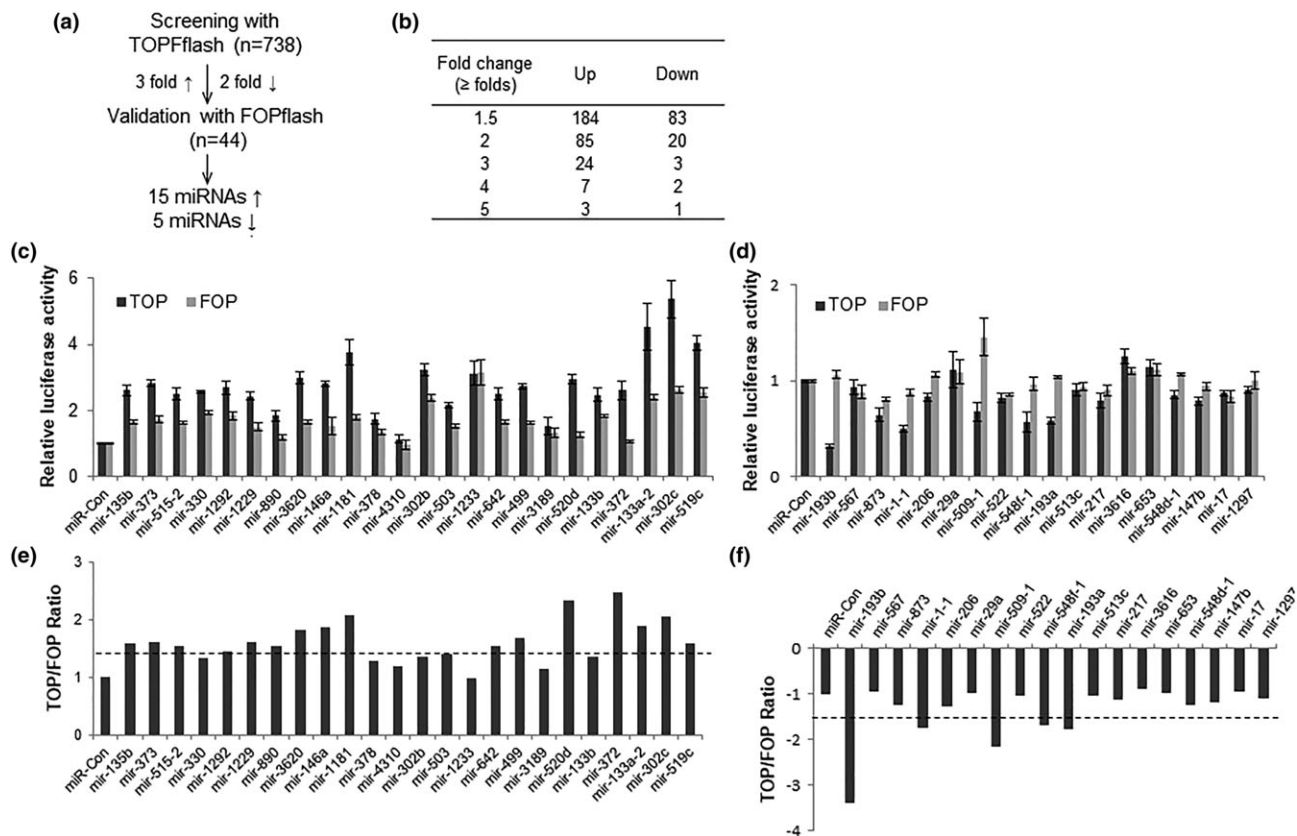
FIGURE 1 Screening of miRNAs regulating Wnt/β-catenin signalling. (a) Schematic of miRNA screening. (b) Summary of miRNA hits in Wnt/β-catenin signalling screening. (c–f) miRNA hit verification. HEK293 cells were transfected with a miRNA plasmid or its control vector (miR-Con) together with the TOPflash (wild-type TCF binding sites) or FOPflash (mutated TCF binding sites) luciferase reporter vector and were stimulated with 50% Wnt3a-conditioned medium. TOPFlash or FOPlash firefly luciferase activity was normalised to pRL-TK *Renilla* luciferase activity. The results are expressed as the ratio of miRNA/miR-Con (c,d) and ratio of TOPflash/FOPflash (e,f). A TOP/FOPflash ratio of ≥1.5 was used as a cut-off value

and miR-509-1) that down-regulated Wnt/β-catenin signalling, miR-193a and miR-193b are isoforms of the same family. Because miR-193b showed greater inhibition of Wnt/β-catenin signalling than miR-193a, we tested the anti-IAV activities of miR-193b and the other miRNAs. We overexpressed each miRNA in HEK293 cells for 24 hr, infected the cells with A/PR/8/34 at a multiplicity of infection (MOI) of 0.01 for 48 hr, and determined viral mRNA and protein expression in infected cells and the titre in the culture medium. The miRNA expression vector contains an enhanced green florescent protein (EGFP) marker, which can be used to monitor the transfection efficiency. EGFP images showed an approximately 75–85% transfection efficiency (Figure 2a), and overexpression of miRNAs was confirmed by real-time polymerase chain reaction (PCR; Figure 2b). Western blot analysis showed that overexpression of miR-193b, miR-548f-1, miR-1-1, and miR-509-1 in HEK293 cells reduced viral NP protein expression by 73 ± 14%, 42 ± 9%, 61 ± 25%, and 35 ± 19%, respectively, and NS1 protein expression by 98 ± 1%, 61 ± 21, 63 ± 18, and 30 ± 15%, respectively (Figure 2c,d). These miRNAs also reduced the mRNA levels of NP, NS1, and PB1 in cells by 30–60% (Figure 2e). Furthermore, progeny virus production in the culture media was suppressed by all of the miRNAs (Figure 2f). Immunostaining of NP revealed that these miRNAs also led to a decrease in IAV-infected cells (Figure 2g). It is noteworthy that miR-509-1 inhibited the Wnt/β-catenin signalling, the second most but merely showed

moderate suppression of the IAV infection, suggesting a possible off-target effect of the miRNA. Taken together, the data showed that the miRNAs that down-regulated the Wnt/β-catenin signalling pathway reduced IAV infection.

2.3 | Further characterisation of the anti-IAV activities of miR-193b

Given that miR-193b suppressed Wnt/β-catenin signalling and the viral mRNA and protein levels more than other miRNAs, we selected miR-193b for further investigation. First, we determined whether the effects of miR-193b on IAV infection were cell type dependent. The lung is the primary site of IAV infection, and thus, we chose human lung epithelial A549 cells for this purpose. Due to the low transfection efficiency of plasmid into A549 cells, we used a lentivirus to overexpress miR-193b. Lentivirus infection efficiencies under our conditions were nearly 100% as revealed by EGFP images (Figure 3a) although the intensities of GPF varied among cells. The miR-193b level, as determined by real-time PCR, was increased 26-fold over miR-Con in A549 cells (Figure 3b). Cell viability was not affected by lentivirus infection as determined by CellTiter Blue assay (Figure 3c). Overexpression of miR-193b reduced the viral NP and NS1 protein levels in both multiple cycle (Figure 3d,e) and single cycle (Figure 3h,i) of
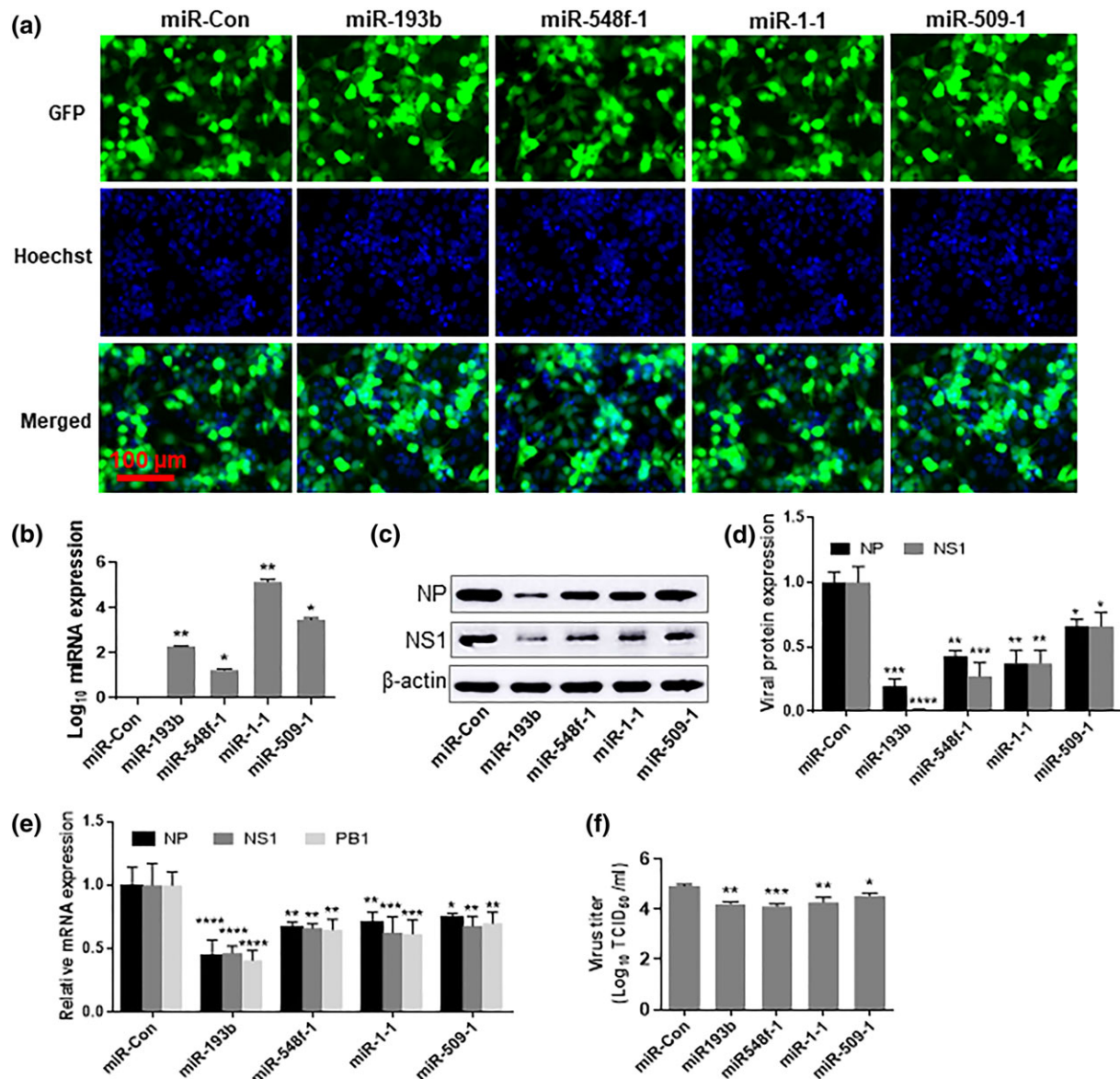
FIGURE 2 Effects of miRNAs that up-regulate Wnt/β-catenin signalling on IAV infection. (a,b) HEK293 cells were transfected with a pENTR-miRNA or its control vector (miR-Con) for 72 hr. The transfection efficiency was monitored by the GFP signal and the cells were counterstained with Hoechst 33342 (blue). miRNA expression was determined by real-time PCR, normalised to β-actin, and expressed as a ratio to miR-Con. (c–f) HEK293 cells were transfected with pENTR-miRNA or miR-con for 24 hr, followed by infection with A/PR/8/34 at an MOI of 0.01 for 48 hr. NP and NS1 protein levels were determined by western blotting, densitometrically quantified and normalised to β-actin. NP, NS1, and PB1 mRNA expression was determined by real-time PCR and normalised to β-actin. Virus yields in the medium were titrated by the TCID$_{50}$ assay. (g) HEK293 cells were transfected with a pENTR-miRNA or miR-con vector for 24 hr, followed by infection with PR8 IAV at an MOI of 0.5 for 16 hr. Immunofluorescent staining was performed to detect viral NP (red). GFP images show cells overexpressing the miRNAs. The cells were counterstained with Hoechst 33342 (blue). Data are expressed as the mean ± SE of three independent experiments. *$P < 0.05$ versus miR-Con, **$P < 0.01$ versus miR-Con, ***$P < 0.001$ versus miR-Con, and ****$P < 0.0001$ versus miR-Con (b and f: one-way ANOVA, Bonferroni's multiple comparisons test; d and e: two-way ANOVA, Bonferroni's multiple comparisons test)

infection. Overexpression of miR-193b also decreased the mRNA levels of NP, NS1, and PB1 by 30% to 43% (Figure 3f) and progeny virus production in the culture medium by more than one log (Figure 3g). These results indicated that the anti-IAV activity of miR-193b was not cell type dependent.

We then assessed whether the effects of miR-193b on IAV infection were dependent on the viral strain using an IAV luciferase reporter assay (More et al., 2018). The IAV luciferase reporter vector contains a firefly luciferase under control of NP 5′ and 3′ UTRs of

influenza A/WSN/33, so it is able to respond to IAV. Luciferase reporter activity was detected after reconstitution of the IAV polymerase complex after virus infection. The reporter vector was transfected into HEK293 or A549 cells along with the miR-193b plasmid or miR-con vector. The cells were then infected with A/PR/8/34, A/WSN/33, OK/09 H1N1, and A/Oklahoma/309/2006 H3N2 at the indicated MOIs for 48 hr, followed by the dual luciferase assay. The viruses were chosen because A/PR/8/34 and A/WSN/33 are the most representative laboratory H1N1 strains, whereas OK/09 is a pandemic
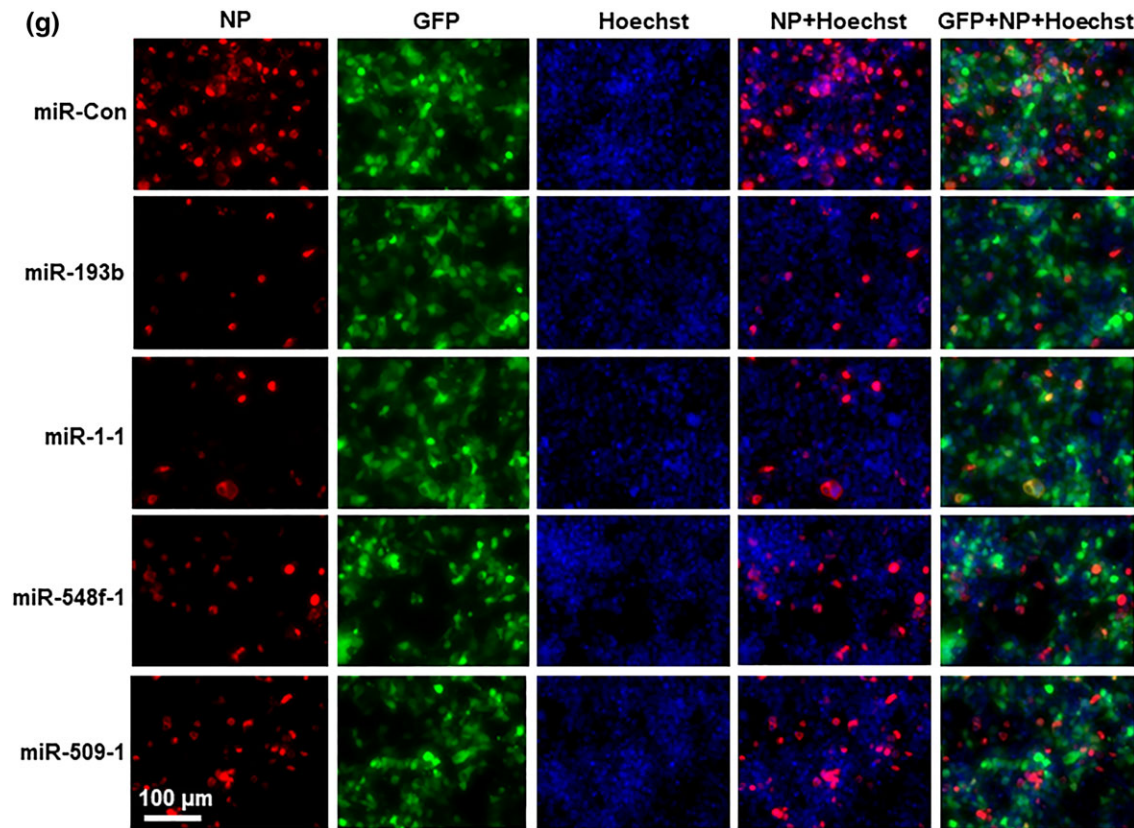
FIGURE 2 Continued

H1N1 virus, and H3N2 is a virus strain that causes seasonal flu annually and endemic outbreaks. To obtain a proper readout of the luciferase activities, we first optimised the dose of the viruses with MOIs of 0.001, 0.005, 0.01, 0.05, and 0.1. The dose that resulted in a ratio (firefly/renilla) between 10 and 100 was selected (data not shown). The results showed that overexpression of miR-193b inhibited IAV infection of all tested strains by 45–73% in HEK293 cells and by 25–76% in A549 cells (Figure 4a,b), indicating that the antiviral effect of miR-193b was not strain dependent.

2.4 | Knockout of miR-193b with CRISPR/Cas9 enhances IAV infection

To determine the effects of endogenous miR-193b on IAV infection, we knocked out miR-193b with CRISPR/Cas9 and determined their effects on IAV infection. Two single guide RNAs (sgRNAs) were designed to target two regions of pre-miR-193b (Figure 5a). A549 cells were infected with a sgRNA-lentiCRISPR virus or a control virus, and one clone was chosen from each sgRNA after puromycin selection. The surveyor mutation assay showed that the mutations were generated in both miR-193b knocked-out clones (Figure 5b). DNA sequencing revealed that one base was inserted in the sgRNA1 clone, and two bases were deleted in the sgRNA2 clone (Figure 5c). miR-193b expression was significantly reduced with both clones (Figure 5d), likely due to the disruption of miRNA processing (Chang et al., 2016). When miR-193b-knocked out A549 cells were infected with A/PR/8/34 at an MOI of 0.01 for 48 hr, viral NP protein level

was significantly increased in both clones (Figure 5e,f). Progeny virus production in the culture medium was increased in the knockout cells but only reaching a significant level in the sgRNA2 clone (Figure 5g). The results further support that miR-193b negatively regulates IAV infection.

2.5 | miR-193b suppresses IAV infection by targeting β-catenin

To determine how miR-193b regulates IAV replication by altering the Wnt/β-catenin signalling pathway, we used PicTar, Target Scan (version 5.2), and DIANA-microT-4.0 to predict the target genes of miR-193b in the pathway. Because miR-193b inhibits Wnt/β-catenin signalling, we narrowed down the target selection to the positive regulators of the signalling. Three positive regulators of the Wnt/β-catenin signalling pathway, LEF1, CTNNB1, and FZD4, were predicted to contain binding sites for miR-193b. FZD4 encodes frizzled 4 protein, which acts as a receptor for Wnt ligands (H. C. Huang & Klein, 2004). LEF1 and CTNNB1 encode the Wnt pathway transcription factor LEF1 and coactivator β-catenin, respectively. Accumulation of β-catenin in the cytoplasm and its eventual translocation into the nucleus act as a transcriptional coactivator of the transcription factor LEF1 (Komiya & Habas, 2008). The potential binding sites between miR-193b and the 3′-UTR of the targets are shown in Figure 6a. To determine whether miR-193b binds these targets, we cloned the 3′-UTRs of these genes into a luciferase reporter and transfected them into HEK293T cells along with the miR-193b
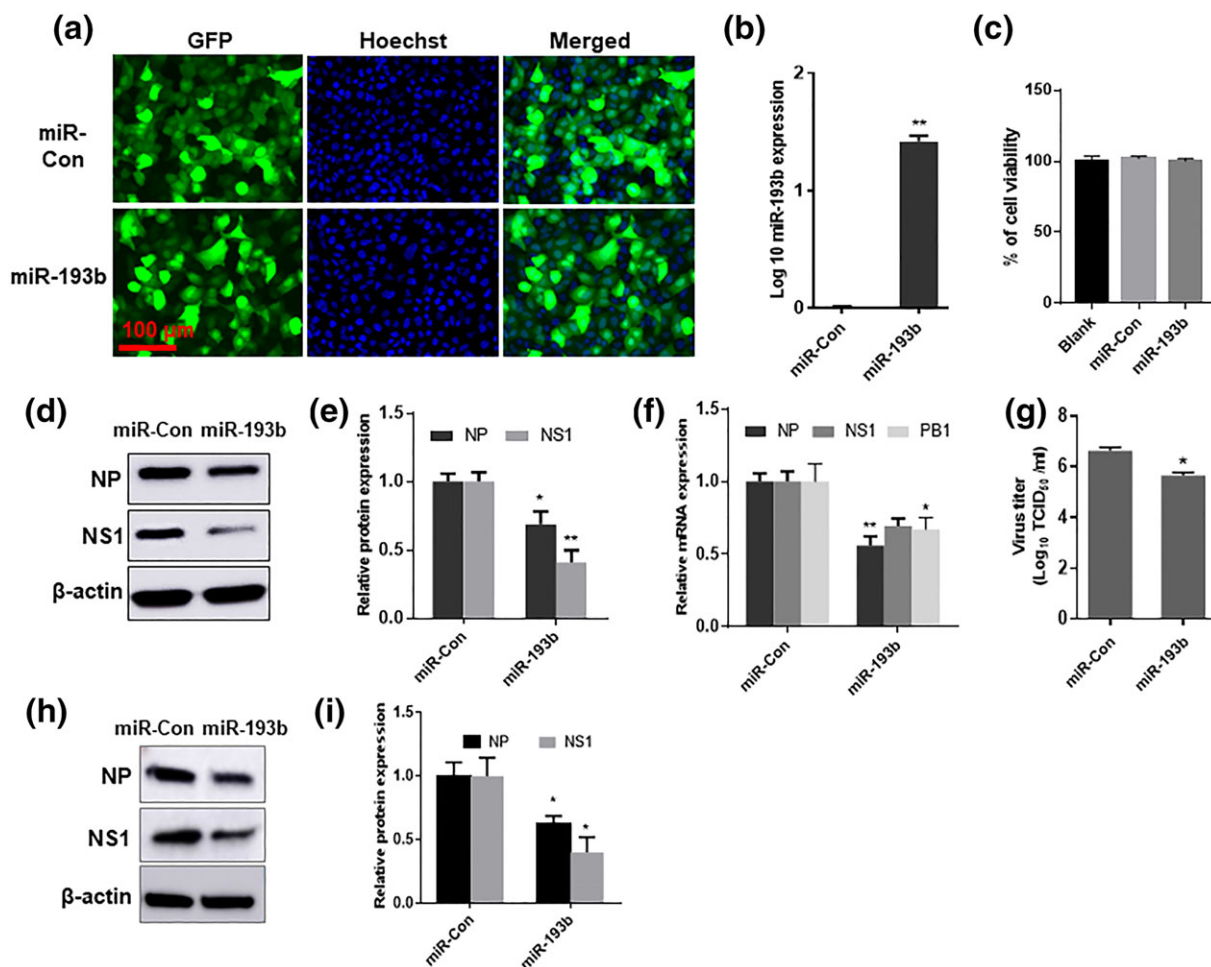
FIGURE 3 Effects of miR-193b on IAV replication in A549 cells. (a,b) Verification of miRNA overexpression. A549 cells were infected with the miR-193b or miR-Con lentivirus at an MOI of 100 for 48 hr. The infection efficiency was monitored by the GFP signal, and the cells were counterstained with Hoechst 33342 (blue). miR-193b expression was determined by real-time PCR and normalised to miR-Con. (c) Cell viability at 72 hr after lentivirus infection determined by a CellTiter Blue assay and normalised to non-infected cells (blank). (d–g) Effects of miR-193b on IAV infection. A549 cells were infected with miR-193b or miR-Con lentivirus (MOI 100) for 48 hr, followed by infection with A/PR/8/34 (MOI 0.01) for 48 hr. NP and NS1 protein expression was detected by western blotting, densitometrically quantified, and normalised to β-actin. Viral NP, NS1, and PB1 mRNA expression was determined by real-time PCR and normalised to β-actin. The virus yield in the medium was titrated by the $TCID_{50}$ assay. (h,i) miR-193b or miR-Con lentivirus-infected A549 cells were infected with IAV at MOI 0.5 for 8 hr. NP and NS1 protein levels in the infected cells were detected by western blotting and quantified. Data are expressed as the mean ± SE of three independent experiments. *$P < 0.05$ versus miR-Con and **$P < 0.01$ versus miR-Con (b and g: Student's t-test; c: one-way ANOVA, Bonferroni's multiple comparisons test; e, f, and i: two-way ANOVA, Bonferroni's multiple comparisons test)
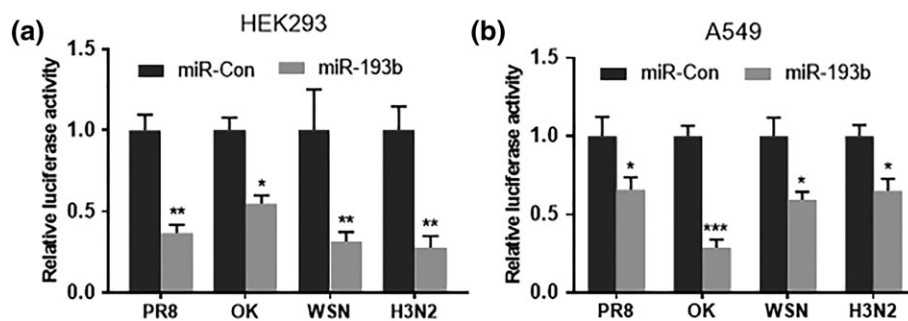
FIGURE 4 Effects of miR-193b on different strains of IAV replication. HEK293 or A549 cells were transfected with a pENTR-miR-193b or control vector (100 ng), the IAV firefly luciferase reporter plasmid vNP-luc/pHH21 (20 ng) and pRL-TK *Renilla* plasmid (5 ng) for 24 hr. The cells were then infected with different strains of IAV, A/PR/8/34, OK/09, A/WSN/33, and A/Wisconsin/67/05 at an MOI of 0.01, 0.05, 0.005, and 0.01, respectively, for 48 hr. Firefly luciferase activity was normalised to pRL-TK *Renilla* luciferase activity in (a) HEK293 and (b) A549 cells. The results are expressed as a ratio to miR-Con-transfected cells. Data shown are the mean ± SE of three independent experiments. *$P < 0.05$ versus miR-Con, **$P < 0.01$ versus miR-Con, and ***$P < 0.001$ versus miR-Con (two-way ANOVA, Bonferroni's multiple comparisons test)
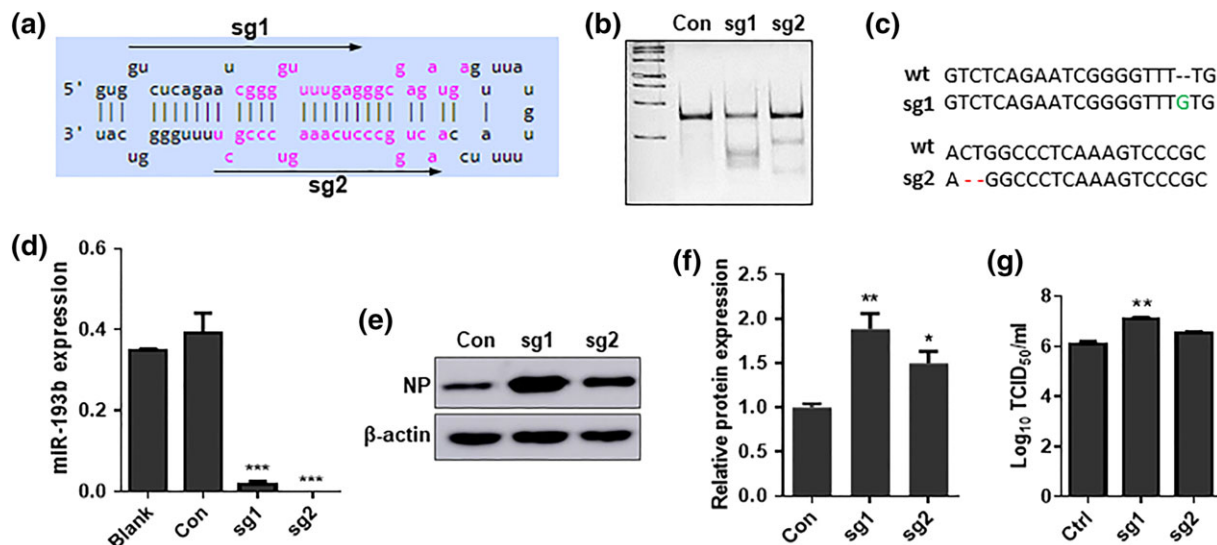
FIGURE 5 Effect of miR-193b knockout on IAV infection. (a) Target regions of two sgRNAs. (b) CRISPR/Cas9-mediated mutation as detected by the surveyor mutation assay. (c) DNA sequencing showing insertion (green) and deletions (red) generated by CRISPR/Cas9 in the miR-193b knocked out clones. (d) miR-193b expression in the miR-193b knocked out clones by CRISPR/Cas9 as determined by real-time PCR. (e–g) sgRNA1, sgRNA2, or control vector (Con)-treated A549 cells were infected with A/PR/8/34 at MOI 0.01 for 48 hr. Viral NP levels were determined with western blotting (e), and densitometrically quantified and normalised to β-actin (f). The progeny virus was determined by $TCID_{50}$ assay (g). *$P < 0.05$ versus Con, **$P < 0.01$ versus Con, and ***$P < 0.001$ versus Con (one-way ANOVA, Bonferroni's multiple comparisons test)

expression plasmid. miR-193b reduced the luciferase activities by 35–50% of all targets (Figure 6b), suggesting that miR-193b was able to bind the 3′-UTRs of LEF1, CTNNB1, and FZD4.

We further examined whether miR-193b reduced endogenous target proteins. HEK293 cells were transfected with the miR-193b plasmid for 48 hr, and western blotting was then performed to evaluate the LEF1, β-catenin, and FZD4 protein levels. The LEF1 and β-catenin protein levels were reduced by 71 ± 6% and 30 ± 2%, respectively, in miR-193b-overexpressing HEK293 cells. However, endogenous FZD4 was not affected by miR-193b overexpression (Figure 6c,d). These results suggest that LEF1 and β-catenin, but not FZD4, are the targets of miR-193b in HEK293 cells. Hereafter, we further examined whether miR-193b also targeted LEF1 and β-catenin in A549 cells. We infected A549 cells with an MOI of 100 of miR-193b lentivirus or the control for 48 hr and detected LEF1 and β-catenin by western blotting. β-Catenin was reduced by overexpression of miR-193b in both of HEK293 and A549 cells (Figure 6e,f). We were unable to detect LEF1 in A549 cells due to its low basal expression. Furthermore, the endogenous β-catenin was elevated in the miR-193b knockout A549 cells, but only sgRNA1 reached a significant level (Figure 6g,h).

To determine whether LEF1 and β-catenin were involved in the anti-IAV activities of miR-193b, rescue experiments were performed by overexpressing target genes using expression vectors that do not contain the 3′-UTR of the target genes. HEK293 cells were cotransfected with miR-193b alone or along with LEF1 or ΔGSK-β-catenin plasmids for 24 hr and then infected with A/PR/8/34 (MOI 0.01) for 48 hr. ΔGSK-β-catenin expresses a stabilised form of β-catenin that has mutations at four GSK3β phosphorylation sites (Ser33, Ser37, Thr41, and Ser45; Barth, Stewart, & Nelson, 1999). Consistent with the previous results (Figure 2), miR-193b reduced endogenous β-catenin protein levels (lower bands) and the NP protein

levels and virus titres in culture media (Figure 7a–c). Ectopic expression of β-catenin was also observed in the ΔGSK-β-catenin-transfected cells (higher bands). The coexpression of ΔGSK-β-catenin and miR-193b abolished the miR-193b-mediated reduction of NP protein level and virus titre. However, coexpression of LEF1 with miR-193b was not able to restore the miR-193b-mediated decreases in NP protein level and progeny virus production (Figure 7d–f). This data suggested that β-catenin was involved in miR-193b-mediated inhibition of IAV replication.

2.6 | miR-193b suppresses cyclin D1 and induces G0/G1 arrest

As a downstream target of Wnt/β-catenin signalling, cyclin D1 plays an important role in the G1-S transition of the cell cycle. Therefore, we further determined whether miR-193b reduced cyclin D1 expression. To this purpose, we transfected HEK293 cells with the miR-193b plasmid or infected A549 cells with miR-193b lentivirus. Real-time PCR and western blotting analyses showed that miR-193b reduced the mRNA and protein levels of cyclin D1 in HEK293 and A549 cells (Figure 8a–c). To determine whether the restoration of cyclin D1 protein level can overcome the inhibition of IAV infection caused by miR-193b, we transfected HEK293 cells with a cyclin D1 expression vector alone or together with a miR-193b expression vector. The results showed that ectopic expression of cyclin D1 abolished the miR-193b-mediated reduction of IAV infection (Figure 8d–f).

To test whether miR-193b was able to affect the cell cycle progression, miR-193b-infected A549 cells were synchronised by cultivation in serum-free medium for 48 hr and then allowed to re-enter the cell cycle by culturing them in medium containing 10% FBS for 18 and 30 hr. The cells were stained with propidium iodide and analysed by
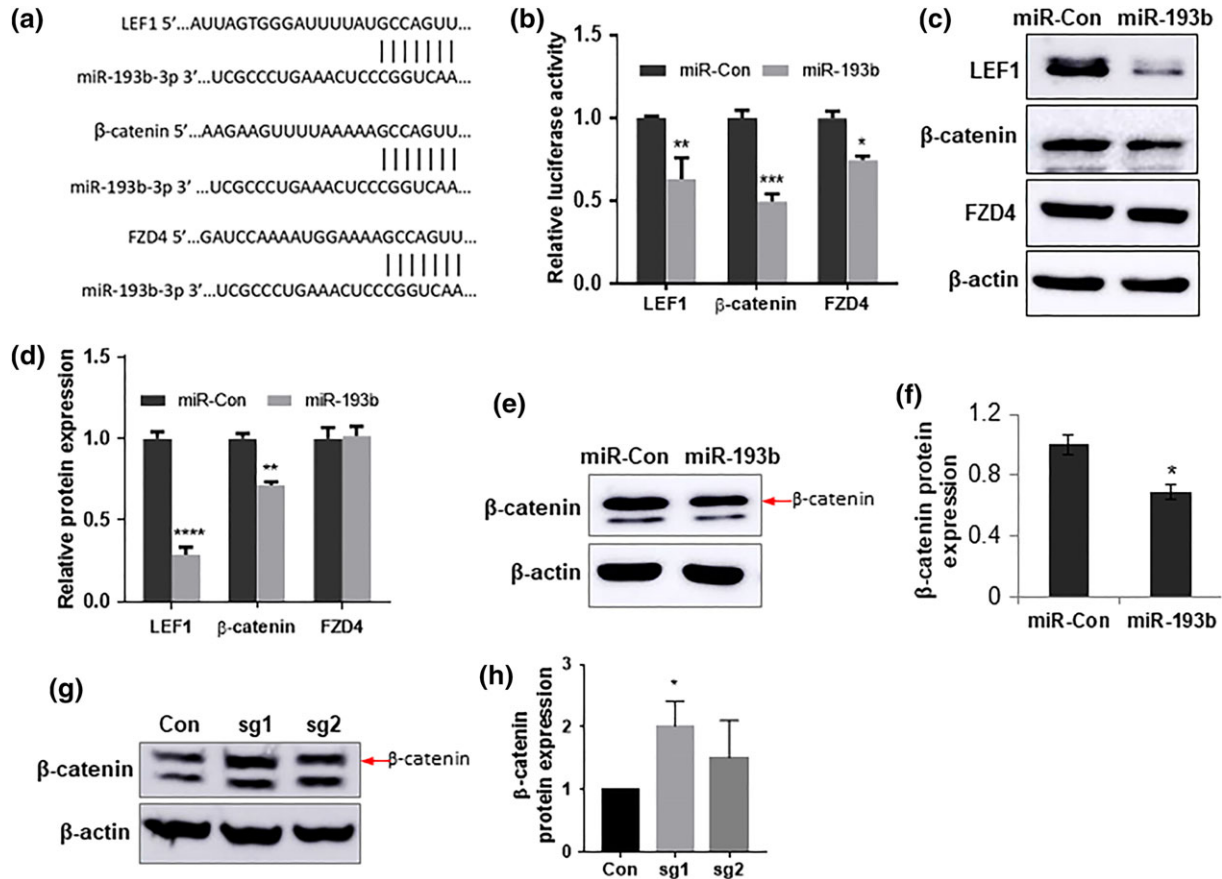
FIGURE 6 miR-193b target verification. (a) Potential interactions between miR-193b and the putative binding sites in the 3′-UTR of LEF1, β-catenin, and FZD4. (b) The 3′-UTR reporter assay. HEK293T cells were transfected with a miR-193b expression vector and a 3′-UTR luciferase reporter plasmid for 48 hr. Firefly luciferase activity was normalised to pRL-TK *Renilla* luciferase activity and then expressed as a ratio to the vector control (miR-Con). (c,d) Effect of miR-193b on endogenous target proteins in HEK293 cells. HEK293 cells were transfected with a miR-193b overexpression plasmid for 48 hr. LEF1, β-catenin, and FZD4 protein expression was detected by western blotting, densitometrically quantified, and normalised to β-actin. (e,f) Effect of miR-193b on endogenous β-catenin in A549 cells. A549 cells were infected with a miR-193b lentivirus for 48 hr. β-catenin protein expression was detected by western blotting, densitometrically quantified, and normalised to β-actin. (g,h) Endogenous β-catenin in miR-193b-knockout A549 cells. β-Catenin protein expression in sgRNA1, sgRNA2, or control vector-treated A549 cells was determined by western blotting and quantified by normalisation to β-actin. Data are expressed as the mean ± *SE* of three independent experiments. *$P < 0.05$ versus miR-Con, **$P < 0.01$ versus miR-Con, ***$P < 0.001$, and ****$P < 0.0001$ versus miR-Con (b and d: two-way ANOVA, Bonferroni's multiple comparisons test; f: Student's *t*-test; h: one-way ANOVA, Bonferroni's multiple comparisons test)

flow cytometry. Approximately 72% of miR-193b-infected cells were in the G0/G1 phase compared with 60–62% of miR-Con-treated cells (Figure 8g) at both time points. On the contrary, miR-193b overexpression decreased the progression of A549 cells to S phase. These data indicated that miR-193b suppressed cyclin D1 expression and inhibited the cell cycle transition from G0/G1 to S.

2.7 | miR-193b hinders the nuclear entry of vRNP

IAV infection involves a complex series of nuclear import and export events. Thus, we examined whether miR-193b was able to inhibit vRNP entry into the nucleus. We infected miR-193b-overexpressing A549 cells with A/PR/8/34 for various times and immunostained the cells with NP antibodies. At 2 hpi, 2% of control cells showed a NP signal in the nucleus compared with almost no signal in the miR-193b-overexpressing cells. At 3 hpi, 57 ± 9% of control cells displayed NP nuclear localisation compared with only 13 ± 4% of the miR-193b-overexpressing cells. At 5 hpi, the proportions of cells

with NP nuclear localisation increased to 93 ± 2% in control cells and 55 ± 9% in miR-193b-overexpressing cells (Figure 9a,b). At 8 hr after infection, most of control and miR-193b-overexpressing cells displayed a NP signal centred in the nuclei. These data suggested that miR-193b delayed vRNP entry into the nucleus.

2.8 | G0/G1 cell cycle arrest inhibits the nuclear entry of vRNP

Because miR-193b induces G0/G1 arrest, we investigated the effect of cell cycle arrest on vRNP nuclear import. G0/G1-arrested A549 cells were obtained by serum starvation in medium containing 0.2% fetal bovine serum (FBS) for 72 hr. Control cells were initially serum-starved for 48 hr and then cultured in complete medium for 24 hr, which allowed the cells to re-enter the normal cell cycle. The cells were then infected at an MOI of 10 of A/PR/8/34 virus for 3 hr, and immunofluorescent (IF) staining was performed to detect viral NP. Ki-67 staining was performed to examine cell cycle arrest. As
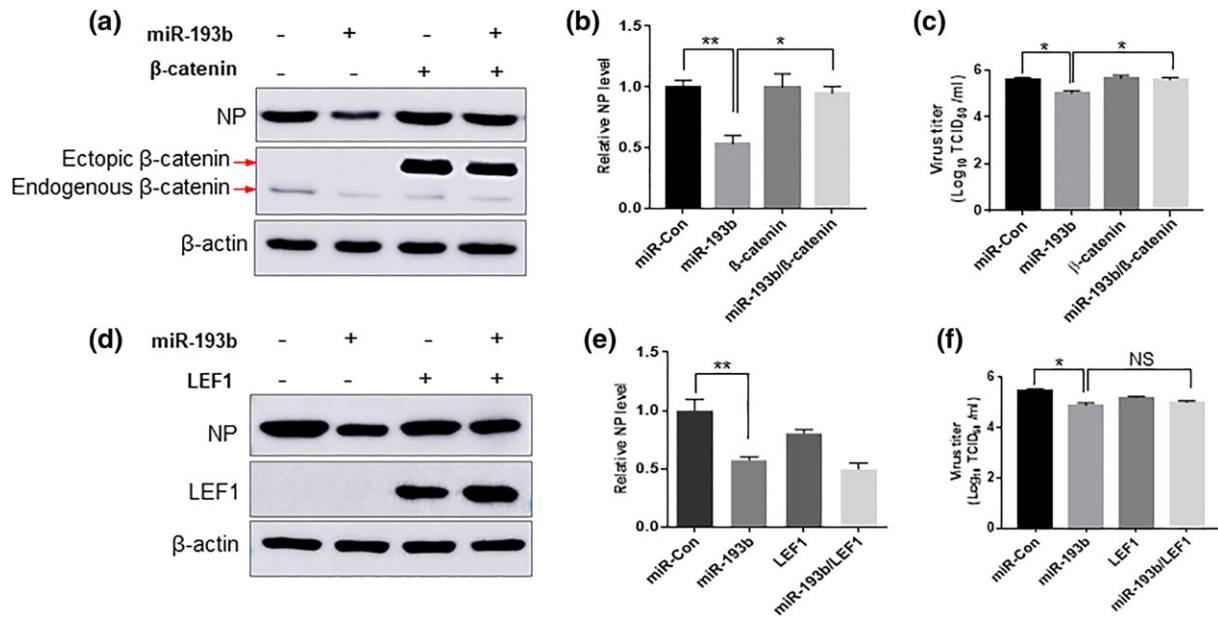
FIGURE 7 β-Catenin is involved in miR-193b-mediated inhibition of IAV infection. HEK293 cells were seeded in 12-well plates and transfected with a miR-193b plasmid (0.5 μg) alone or (a–c) along with pCMV-ΔGSK-β-catenin (β-catenin; 0.5 μg) or (d–f) together with pCS2-LEF-1 (0.25 μg). The cells were then infected with A/PR/8/34 (MOI 0.01) for 48 hr. NP protein expression was detected by western blotting (a,d), quantified and normalised to β-actin (b,e). Progeny virus was determined by TCID$_{50}$ assay (c,f). Data are expressed as the mean ± SE of three independent experiments. *P < 0.05 and **P < 0.01 (one-way ANOVA, Tukey's multiple comparison test). NS: not significant
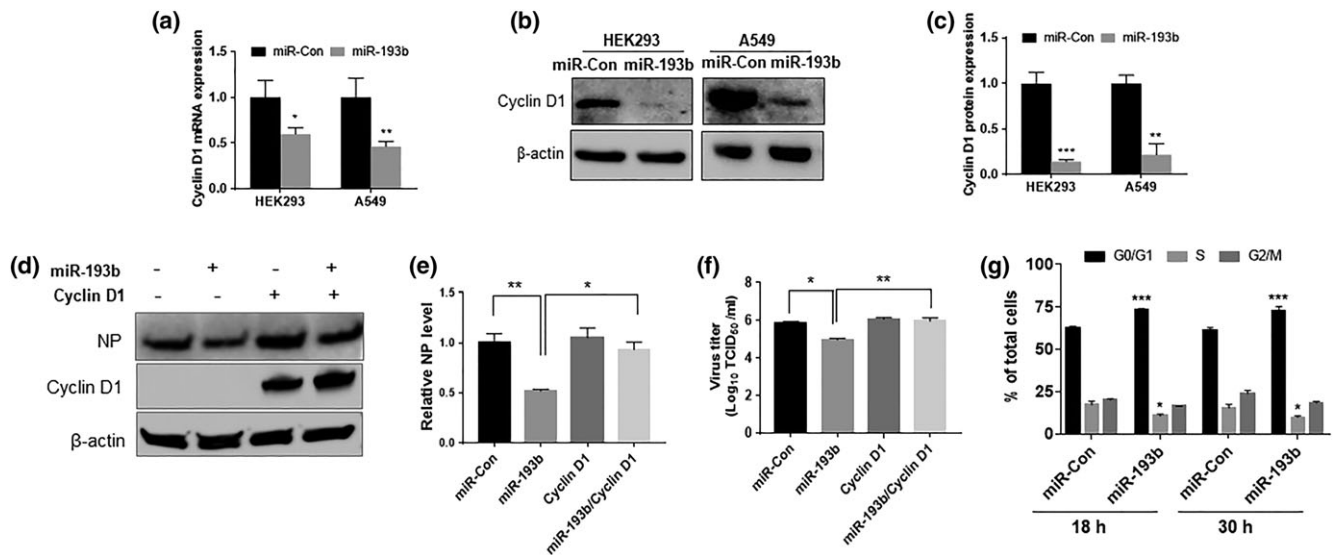
FIGURE 8 miR-193b suppresses cyclin D1 and induces G0/G1 cell cycle arrest. (a–c) HEK293 cells were transfected with a miR-193b expression plasmid for 48 hr, or A549 cells were infected with a miR-193b lentivirus (MOI 100) for 48 hr. The mRNA (a) and protein (b) levels of cyclin D1 were detected by real-time PCR and western blotting, respectively. Protein expression was densitometrically quantified and normalised to β-actin (c). (d–f) HEK293 cells were seeded in 12-well plates and transfected with a miR-193b plasmid (0.5 μg) alone or along together with p-CMV-CCND1 (0.5 μg, Addgene #19927) expression plasmid. The cells were then infected with A/PR/8/34 (MOI 0.01) for 48 hr. NP protein expression was detected by western blotting, quantified, and normalised to β-actin. Progeny virus was determined by TCID$_{50}$ assay. (g) miR-193b lentivirus-infected A549 cells were serum-starved for 24 hr and then cultured in medium containing 10% fetal bovine serum for 18 and 30 hr. The cells were stained with propidium iodide. The DNA content was measured by flow cytometry. The cell cycle phase distribution was examined. Data are expressed as the mean ± SE of three independent experiments. (a,c, and g) *P < 0.05 versus miR-Con, **P < 0.01 versus miR-Con (two-way ANOVA, Bonferroni's multiple comparisons test). (e and f) *P < 0.05 and **P < 0.01 (one-way ANOVA, Tukey's multiple comparison test)

shown in Figure 10a,b, the fluorescence signal of Ki-67, a marker for cell proliferation, was significantly reduced in serum-starved cells compared with the control. By contrast, NP nuclear translocation

was 2.3-fold higher in control cells than in the cells that were in G0/G1 cell cycle arrest. These data indicated that G0/G1 cell cycle arrest indeed suppressed vRNP entry into the nucleus.
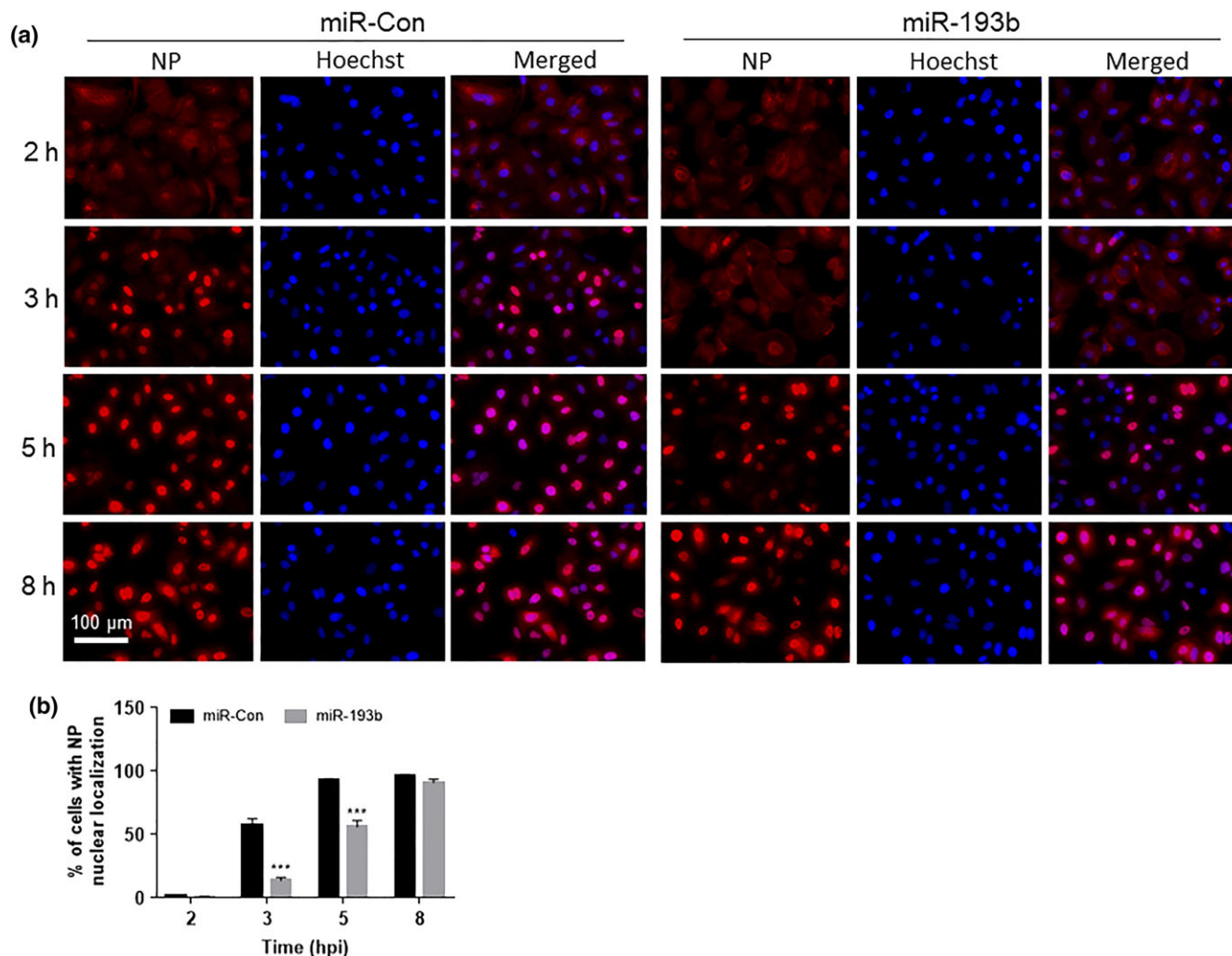
FIGURE 9 miR-193b suppresses IAV vRNP nuclear import. (a) miR-193b or miR-Con lentivirus-infected A549 cells were infected with A/PR/8/34 at an MOI of 10 for 2, 3, 5, and 8 hr. Viral NP (red) was immunostained, and the nuclei (blue) were counterstained. (b) Cells with intense NP signal localised (centred) in the nucleus were considered to exhibit nuclear localisation and counted. The percent of cells with NP nuclear localisation at different times was quantified. Data are expressed as the mean ± *SE* of three independent experiments. ***$P < 0.001$ versus miR-Con (two-way ANOVA, Bonferroni's multiple comparisons test)

2.9 | IAV infection causes down-regulation of miR-193b in vitro

To assess the effect of IAV infection on miR-193b expression, A549 or HEK293 cells were infected with A/PR/8/34 at MOI 0.01 for 0, 24, 48, and 72 hr. As determined by real-time PCR, the expression level of miR-193b shows a trend in reduction with time of infection and reached a significant decrease at 72 hr post infection in both A549 and HEK293 cells (Figure 11), suggesting that IAV infection may counteract the miR-193b expression.

2.10 | miR-193b suppresses viral infection in mice challenged with a sublethal dose of A/PR/8/34

To determine whether miR-193b inhibited IAV replication in vivo, we overexpressed miR-193b in the lungs of mice using an adenoviral vector, challenged mice with a sublethal dose of A/PR/8/34 (250 PFU/mouse), and examined the body weight and viral mRNA and progeny virus production in lung tissues at Days 3 and 7 post infection. No mortality was observed in either control or miR-193b-treated mice. Body weight loss was slightly improved in miR-193b-treated mice (Figure 12a). As determined by real-time PCR, the miR-193b levels in lung tissues were approximately 22-fold and six-fold higher than those in the control at Days 3 and 7 post infection, respectively (Figure 12b). The decrease in miR-193b expression from Day 3 to Day 7 was likely due to transient expression of miR-193b by the adenovirus vector. Cyclin D1 mRNA was clearly suppressed in the lung of the mice overexpressing miR-193b (Figure 12c). Viral NP mRNA was significantly reduced by overexpression of miR-193b in the lungs of mice at Day 7 post infection (Figure 12d). Progeny virus production in the lungs was also decreased at 7 dpi although it did not reach a significant level (Figure 12e). Taken together, these results confirm the antiflu activities of miR-193b in vivo.
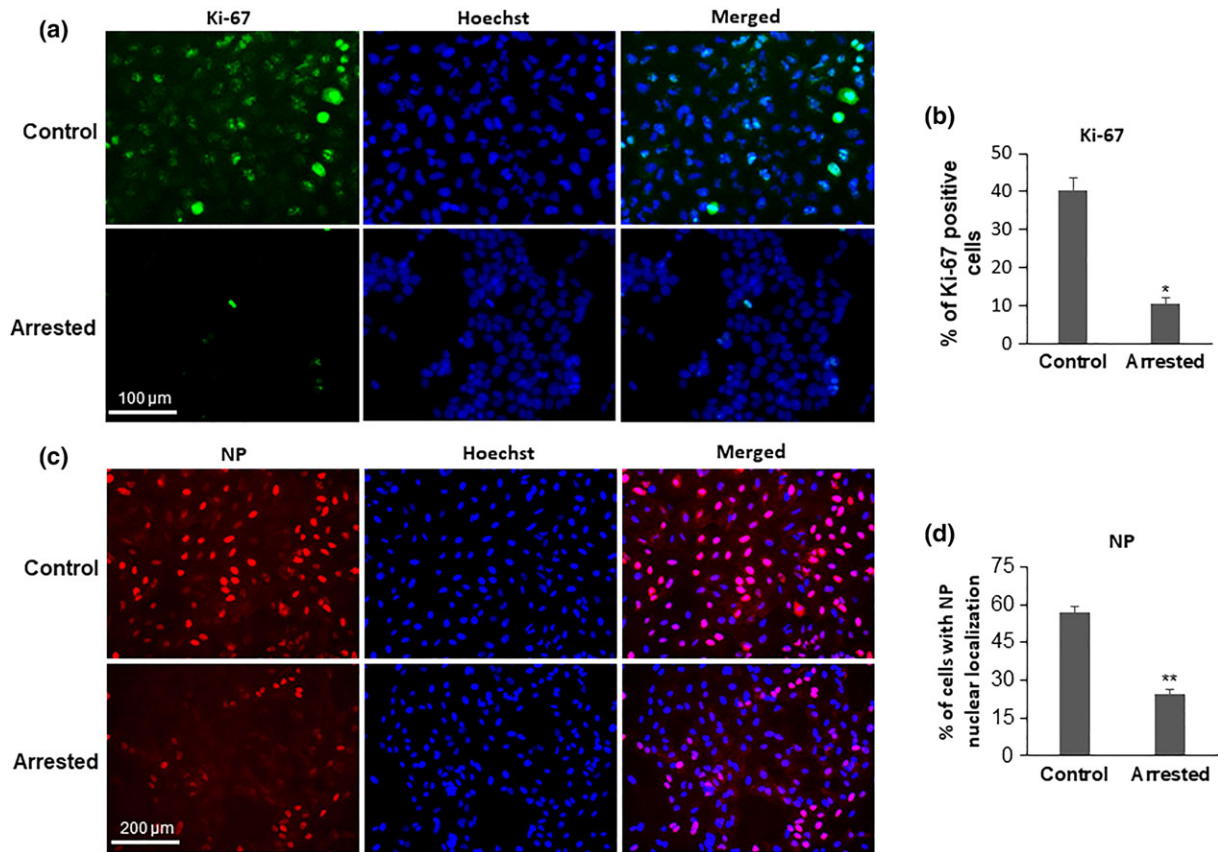
FIGURE 10 Effect of G0/G1 cell cycle arrest on IAV NP nuclear import. G0/G1-arrested A549 cells were achieved by culturing the cells in medium containing 0.2% of fetal bovine serum for 72 hr. Control cells were first serum-starved in medium containing 0.2% fetal bovine serum for 48 hr and then cultured in complete medium (containing 10% fetal bovine serum) for 24 hr to allow them to enter the normal cell cycle. (a) Ki-67 was immunostained (green), and cell nuclei were counterstained (blue). (b) Quantification of Ki-67 positive cells. (c) Control or arrested cells were infected with A/PR/8/34 (MOI of 10) for 3 hr. Immunofluorescence staining was performed to detect viral NP (red). The cells were counterstained with Hoechst 33342 (blue). (d) The percent of cells with NP nuclear localisation was quantified. Data are expressed as the mean ± SE of three independent experiments. *P < 0.05 versus control, **P < 0.01 versus control (Student's t-test)
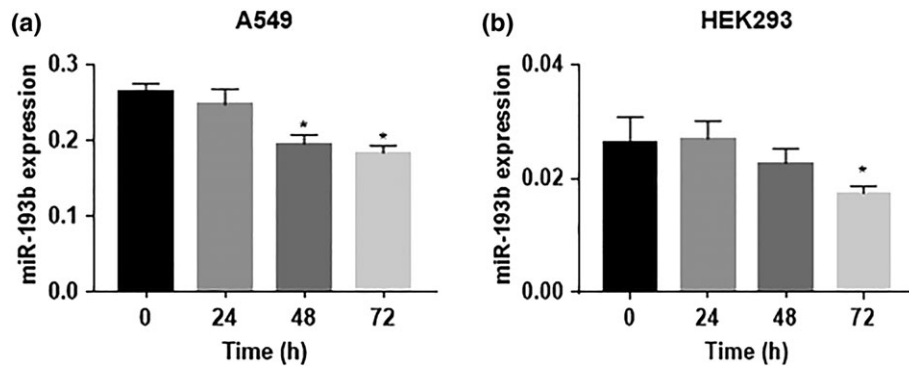
FIGURE 11 Effect of IAV infection on miR-193b expression. (a) A549 or (b) HEK293 cells were infected with A/PR/8/34 (MOI 0.01) for 0, 24, 48, and 72 hr. miR-193b expression in the cells was determined by real-time PCR and was normalised to U48. *P < 0.05 versus 0 hr (one-way ANOVA, Bonferroni's multiple comparisons test)

3 | DISCUSSIONS

As influenza pathogenesis is determined in part by the host response, understanding the key host modulators of viral infection and virus-induced disease is a promising approach to host-oriented drug development for preventing the disease. The Wnt/β-catenin signalling pathway has been shown to play an important role in virus replication

(More et al., 2018; Shapira et al., 2009) and virus-induced immune responses (Hillesheim, Nordhoff, Boergeling, Ludwig, & Wixler, 2014). Identification of miRNAs that interfere with IAV replication by modulating Wnt/β-catenin will provide new insights into the miRNA-Wnt/β-catenin signalling-IAV interaction network. In the present study, using miRNA library screening, we identified 15 and five miRNAs that up- and down-regulated Wnt/β-catenin signalling,
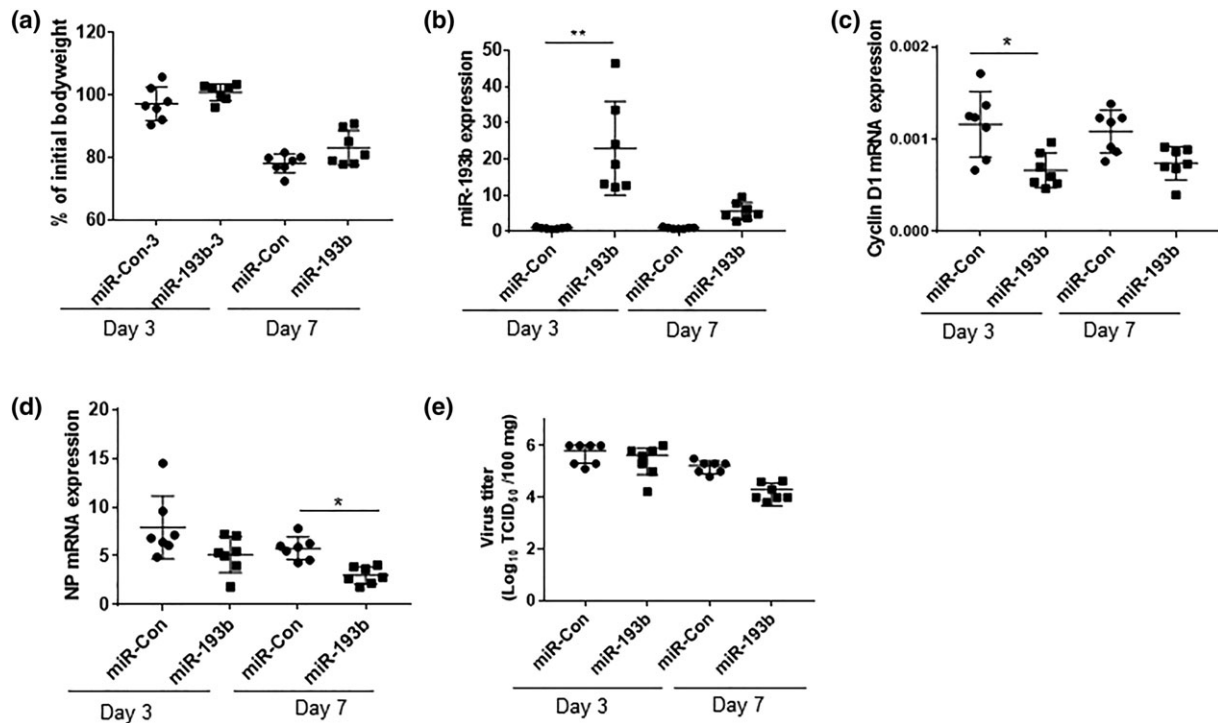
FIGURE 12 miR-193b suppresses viral infection in mice challenged with a sublethal dose of A/PR/8/34. Two days after receiving 10^9 IFU of adenoviral miR-193b or miR-Con, C57BL/6J mice were infected with A/PR/8/34 (250 PFU/mouse). Mice were euthanised at Day 3 or 7 post infection. (a) Percent of body weight normalised to the initial body weight ($n = 7$). (b) miR-193b expression in the lungs of mice at Day 3 or 7 post infection was determined by real-time PCR, normalised to β-actin, and expressed as a ratio to miR-Con on the corresponding days ($n = 7$). (c) Cyclin D1 mRNA expression was determined by real-time PCR and normalised to β-actin ($n = 7$). (d) Viral mRNA levels were detected by real-time PCR and normalised to β-actin ($n = 7$). (e) Virus progeny production in lung homogenate was determined by $TCID_{50}$ assay ($n = 7$). The data are presented as the mean ± SD. *$P < 0.05$ versus miR-Con and **$P < 0.01$ versus miR-Con on the corresponding days (nonparametric Friedman's two-way ANOVA, Bonferroni's multiple comparisons test)

respectively (Figure 1 and Table S1). Furthermore, four miRNAs (miR-193b, miR-548f-1, miR-1-1, and miR-509-1) that down-regulated the Wnt/β-catenin signalling pathway were shown to suppress IAV replication and virus production. miR-193b, which reduced Wnt/β-catenin pathway signalling most significantly, showed the highest inhibition of viral mRNA and proteins in vitro (Figure 2). Furthermore, mice overexpressing miR-193b in the lung by adenoviral delivery benefited from less bodyweight loss and viral load after challenge with a sublethal dose of A/PR/8/34 virus (Figure 12).

Emerging evidence supports the importance of miRNA-mediated gene regulation of the Wnt/β-catenin signalling pathway. A number of miRNAs regulate Wnt signalling by modulating Wnt ligands, β-catenin, transcription factors, and the destruction complex. For example, miR-22, -200b, -185, -26a, -329, and -410 target Wnt ligands to inhibit the Wnt/β-catenin signalling pathway (G. Li et al., 2014; Shiah et al., 2014; Tang et al., 2013; Z. Wang, Humphries, Xiao, Jiang, & Yang, 2014; Zhao et al., 2014). The miR-200 cluster targets β-catenin to inhibit cancer progression (J. Liu et al., 2013; Tian et al., 2014). miR-155 negatively regulates APC in multiple carcinomas, including HCC and papillary thyroid carcinoma (X. Zhang et al., 2013), to promote cell proliferation and tumorigenesis. In the present study, we found that miR-193a/b, miR-548f-1, miR-1-1, and miR-509-1 significantly repressed Wnt/β-catenin signalling. Excluding miR-1, which has been previously reported (Anton et al., 2011), miR-193b, miR-548f-1, and miR-509-1 are newly identified negative regulators

of Wnt/β-catenin signalling. miR-1-1 and miR-133a-2 are members of a cluster family. They are encoded at two paralogous loci and are reported to down-regulate and display tumour-suppressive functions in various human cancers (Hudson et al., 2012; Kojima et al., 2012; Nasser et al., 2008). miR-509-1, previously named miR-509, inhibits cell proliferation and migration in multiple carcinomas (B. Liu et al., 2015; Ma et al., 2016; W. B. Zhang, Pan, Yang, & Zheng, 2013).

All of the four miRNAs that inhibit Wnt/β-catenin signalling reduced viral protein levels. It is noted that to the extent that a miRNA inhibits Wnt/β-catenin signalling does not exactly correlate with its anti-influenza virus activities (Figures 1f and 2d). It is likely that, in addition to Wnt/β-catenin signalling, these miRNAs also target other pathways. Among the down-regulating miRNAs, miR-193b was the most effective suppressor of the Wnt/β-catenin signalling pathway. miR-193b is considered to be a biomarker of various cancers because it is down-regulated in lung cancer (H. Hu, Li, Liu, & Ni, 2012), hepatocellular carcinoma (Xu et al., 2010), prostate cancer (Rauhala et al., 2010), and melanoma (Chen et al., 2010). By contrast, miR-193b has been demonstrated to suppress carcinoma cell proliferation, migration, invasion, and metastasis (Leivonen et al., 2009; Wu, Lin, Zhuang, & Liang, 2009), suggesting that miR-193b may function as a tumour suppressor. Excluding hepatitis B virus-associated hepatocellular carcinoma (Mao et al., 2014), the role of miR-193b in modulating viral infection has rarely been studied to date. In this study, we found that miR-193b strongly suppressed IAV infection. We further

demonstrated that miR-193b inhibited IAV infection by targeting and repressing β-catenin (Figures 6 and 7). To the best of our knowledge, this is the first report to show that miR-193b possesses antiviral activities.

During virus infection, various cellular signalling cascades are activated, which may support or inhibit viral replication. One important signalling pathway that modulates viral replication is the canonical Wnt/β-catenin pathway. Two recent genome-wide siRNA screens identified multiple components of the Wnt pathway that interfere with Rift Valley fever virus and flavivirus infection (Harmon et al., 2016; Smith, Jeng, McWeeney, & Hirsch, 2017). Previous studies have also shown that the deletion of Wnt pathway components significantly impacts IAV replication and interferon production (Shapira et al., 2009; Watanabe et al., 2014). β-Catenin is a part of adherens junctions at the cell membrane and acts as a transcription factor that interacts with LEF/TCF to regulate the Wnt/β-catenin pathway. Increasing evidence has suggested the importance of β-catenin in viral replication, but some discrepancies exist. Hillesheim et al. (2014) showed that β-catenin accumulates in the nucleus after IAV infection and that β-catenin supports IRF3-dependent transcription of genes responsible for the cellular innate immune response, such as IFN-β and ISGs. By contrast, Baril et al. (2013) reported that infection by SeV, another negative-strand RNA virus, induces secretion of Wnt ligands and stabilisation of β-catenin and decreases expression of IFNB1 via a feedback mechanism. Our study showed that the reduction of β-catenin by miR-193b indeed hampered IAV replication and that compensating β-catenin by β-catenin ectopic expression restored IAV infection (Figure 7). Similarly, Watanabe *et al.* showed that down-regulation of β-catenin significantly decreased the relative viral RNA polymerase activity by more than 50% (Watanabe et al., 2014). Although the reasons for the discrepancy in regard to the roles of β-catenin in the RNA virus-induced interferon response and virus infection are not known, different post-translational modifications of the β-catenin protein due to the different Wnt stimuli and the different viruses and cell types used might be plausible explanations.

LEF1 is also a target of miR-193b. However, LEF1 co-overexpression with miR-193b plasmid did not rescue the miR-193b-mediated reduction of IAV infection. LEF1 forms a complex with β-catenin to activate the Wnt/β-catenin responsive genes. Two reports have shown that whereas overexpressing LEF1 alone does not activate the Wnt/β-catenin signalling pathway, coexpression of LEF1 and β-catenin results in 50- to 100-fold increases in the TOPFlash activity (Ahrens, Romereim, & Dudley, 2011; Ishitani, Matsumoto, Chitnis, & Itoh, 2005). It has also been reported that Drosophila TCF activates gene transcription in the presence of Armadillo, the Drosophila homologue of β-catenin. However, Drosophila TCF actually functions as a repressor in the absence of Armadillo (Cavallo et al., 1998; de Lau & Clevers, 2001). This may explain why LEF1 overexpression alone even resulted in a decrease of IAV NP protein expression and virus production (Figure 7d–f). Furthermore, β-catenin has a transactivation domain but not LEF-1 (Vleminckx, Kemler, & Hecht, 1999). These studies suggest that LEF1 requires β-catenin for its transcription activation activity. Because miR-193b reduces the protein levels of both β-catenin and LEF1, overexpression of LEF1 alone cannot rescue the miR-193b effects on IAV infection.

Because miR-193b inhibits both Wnt/β-catenin signalling and influenza virus infection, we focused our target identification of miR-193b on positive regulators of the Wnt/β-catenin pathway. However, we cannot rule out the possibility that miR-193b may also act on other targets and pathways. There are several reported targets of miR-193b in different cells. For example, miR-193b targets ETS1 transcription factor to cause cell cycle arrest and to inhibit the invasion and migration of hepatoma cells (Xu et al., 2010). Up-regulation of c-Kit oncogene frequently occurs in subsets of acute myeloid leukaemia (AML). Overexpression of miR-193b in the Kasumi-1 acute myeloid leukaemia cell line decreases c-Kit expression and inhibits the downstream PDK1/Akt signalling pathway (Gao et al., 2011). miR-193b also targets the urokinase-type plasminogen activator (uPA), an enzyme involved in the degradation of extracellular matrix proteins, resulting in the repression of tumour progression and invasion in human breast cancer (X. F. Li, Yan, & Shao, 2009). Last but not the least, miR-193b induces G1-phase arrest in pancreatic ductal adenocarcinoma by targeting KRAS, through which the AKT and ERK pathways were modulated (Jin et al., 2015).

A good number of studies suggest that crosstalk occurs between the cell cycle and Wnt signalling. It has been well demonstrated that Wnt/β-catenin signalling stimulates the G1/S transition and promotes cell cycle progression and therefore proliferation through transcriptional up-regulation of target genes that encode, for example, c-Myc and cyclin D (Niehrs & Acebron, 2012). By contrast, the β-catenin levels increase during the G1/S transition and peak during G2/M in normal and transformed epithelial cells (Olmeda, Castel, Vilaro, & Cano, 2003). It was recently found that the mitotic CDK14/cyclin Y complex promotes Wnt/β-catenin signalling through phosphorylation of the LRP6 coreceptor (Davidson & Niehrs, 2010). Cyclin D1 is a major regulator of the progression of cells into the proliferative stage of the cell cycle and is necessary for cells to enter S phase (Baldin, Lukas, Marcote, Pagano, & Draetta, 1993). Down-regulation of cyclin D1 induces G0/G1 arrest (Masamha & Benbrook, 2009; Radu, Neubauer, Akagi, Hanafusa, & Georgescu, 2003). We observed that cyclin D1 is markedly down-regulated in miR-193b-overexpressing cells. This is likely due to the combined effect of a reduced Wnt/β-catenin signalling activity and a direct repression by miR-193b because cyclin D1 is a well-known down-stream target of Wnt/β-catenin signalling (Shtutman et al., 1999), and cyclin D1 has been previously shown to be a direct target of miR-193 in cancer cells (Chen et al., 2010).

Based on the observations that miR-193b reduced cyclin D1 protein levels and induced cell cycle G0/G1 arrest, and that miR-193b and cell cycle G0/G1 arrest suppressed viral vRNP nuclear import, we speculate that miR-193b may inhibit vRNP nuclear import by minimising the cell cycle conditions needed for efficient viral nucleoprotein expression and/or transport. The correlation of the cell cycle and viral replication has been reported. For instance, some DNA viruses promote quiescent cells entry into S phase to support viral genome synthesis. By contrast, some large DNA viruses and RNA viruses can arrest cells in a particular phase of the cell cycle that is favourable for replication of a specific virus (Bagga & Bouchard, 2014; Emmett, Dove, Mahoney, Wurm, & Hiscox, 2005). Another mechanism may be related to cellular traffic. For example, Cawood,

Harrison, Dove, Reed, and Hiscox (2007) demonstrated that the nucleocapsid protein of Coronavirus is more mobile in proliferative cells and localises to the nucleolus in a cell cycle-dependent manner. The trafficking of viral proteins may depend on the dynamics of the nucleolar proteome in response to the metabolic profile of the cell. It is noted that two studies suggest that cell cycle G0/G1 arrest facilitates IAV infection (He et al., 2010; Jiang et al., 2013).

In summary, herein, we identified several miRNAs as novel negative regulators of Wnt/β-catenin signalling. miR-193b possesses potent anti-influenza virus activities. The inhibitory effect of miR-193b on IAV infection occurs through inhibition of β-catenin, likely by inducing cell cycle arrest. This discovery may facilitate the identification of potential targets for anti-influenza therapeutics and drug discovery.

4 | EXPERIMENTAL PROCEDURES

4.1 | Cells and viruses

Human lung epithelial A549 cells (American Type Culture Collection, ATCC, Manassas, VA, USA) were maintained in F-12K medium supplemented with 10% FBS and 1% penicillin and streptomycin (P/S). Madin-Darby Canine Kidney (MDCK, ATCC) epithelial, human embryonic kidney (HEK) 293 and HEK293T (ATCC) cells were maintained in Dulbecco's modified Eagle's medium (DMEM) containing 10% FBS and 1% P/S.

Influenza A/Puerto Rico/8/34 (A/PR/8/34) H1N1 virus, a well-characterised mouse adapted laboratory strain, and influenza 2009 pandemic clinic isolate A/Oklahoma/3052/09 (OK/09) H1N1 virus were propagated in the allantoic cavity of 10-day-old embryonated chicken eggs (Charles River Laboratories, MA, USA). Influenza A/WSN/1933 (A/WSN/33) H1N1 virus and A/Oklahoma/309/2006 (A/Oklahoma/309/06) H3N2 virus were propagated in MDCK cells.

4.2 | Cell viability assay

Cell viability was determined by using a CellTiter Blue Cell Viability assay kit (Promega, Madison, WI, USA) according to the manufacturer's instructions. Cells were cultured in 96-well plates and were incubated with the CellTiter Blue Reagent at 37°C for 2 hr. Fluorescence was measured using an excitation at 560 nm and an emission at 590 nm on a plate reader.

4.3 | miRNA expression library construction

The miRNA overexpression vectors contained the CMV promoter, followed by an EGFP tag, a mature miRNA with flanking sequences (~200 bp at each end), and the SV40 poly(A) terminal sequence. Mature miRNAs plus flanking sequences were amplified from human genomic DNAs and cloned via Xho I and EcoR I sites into a modified pLVX-Puro lentiviral vector (Clontech, Mountain View, CA, USA) or a modified pENTR vector between EGFP and SV40 poly(A) terminal sequence, as previously described (Bhaskaran et al., 2009; C. Huang et al., 2017). Inserted vector with a similar size of genomic DNA that did not contain any miRNAs or stem loop structures was used as a control (miR-con).

4.4 | High-throughput miRNA screening

A TOPflash reporter vector containing three copies of TCF/LEF binding sites upstream of the thiamine kinase minimal promoter and firefly luciferase gene (Upstate Biotechnology, Inc., Lake Placid, NY) was used to monitor the Wnt/β-catenin activity. HEK293T cells were seeded in antibiotic-free culture medium in 96-well plates (2×10^4 cells per well). At 20 hr after seeding, the cells were transfected with a TOPflash vector (20 ng), a pLVX-Puro lentiviral miRNA or control plasmid (miR-Con; 100 ng), and a normalisation pRL-TK vector (0.2 ng), using Lipofectamine 2000 (Thermo Fisher Scientific, Waltham, MA, USA). At 20 hr post transfection, the cells were stimulated with Wnt3a conditioned medium (50%; Guo et al., 2014) for 24 hr and lysed in 70-μl passive lysis buffer (Promega, Madison, WI, USA) for 20 min. After a brief centrifugation (12,000 ×g for 5 min at 4°C), the supernatant was collected. Forty microlitres of firefly and 40 μl of *Renilla* luciferase reagents were dispensed into each well of a 96-well plate, in which 10 μl of the collected supernatant had been previously added. Readings were collected using a plate luminometer (BMG LABTECH, Cary, NC, USA). Primary screening was performed in triplicate in a 96-well plate. Firefly luciferase activities in lysates were normalised to those of *Renilla* luciferase. The results are expressed as ratios of the relative luciferase activities over miR-Con. To verify the results, the positive hits from the initial screening were screened for the second time using a TOPflash vector and a FOPflash containing the mutated LEF-1 binding sites under the same conditions as in the primary screening.

4.5 | MiRNA target prediction

The bioinformatics prediction tools PicTar (http://pictar.mdc-berlin.de/), Target Scan (version 5.2; http://www.targetscan.org/), and DIANA-microT-4.0 (http://diana.imis.athena-innovation.gr/) were used to identify potential targets of miR-193b.

4.6 | Construction of 3′-UTR luciferase reporter vectors and the IAV reporter vector

The 3′-UTRs of predicted target genes of the miRNAs were PCR-amplified and inserted into the pmirGLO dual-luciferase miRNA target expression vector (Promega, Madison, WI) at the NheI and SalI sites.

To detect IAV infection with a luciferase reporter assay, we constructed an IAV reporter vector encoding firefly luciferase under control of the 3′-UTRs of the influenza A/WSN/33 NP segment as previously described (Lutz, Dyall, Olivo, & Pekosz, 2005). Briefly, the 3′- and 5′-UTRs of the influenza A/WSN/33 NPs were amplified by PCR and inserted into the RNA polymerase I promoter/terminator cassette of the pHH21 vector (a kind gift from Dr. Yoshi Kawaoka, U. Wisconsin) at BsmB I sites (pHH21-NP-3′-UTR-LUC-NP-5′-UTR).

All inserts were confirmed by DNA sequencing.

4.7 | Production of miRNA lentivirus or adenovirus

A lentiviral vector was cotransfected with psPAX2 and pMD2G (Cellecta, Mountain View, CA, USA) into HEK293T cells using polyethylenimine (PEI, Sigma, St. Louis, MO, USA; 6 μg PEI/μg plasmid) to generate lentivirus expressing miR-193b or the control. The pENTR-miRNA vector or miR-con was switched into an adenovirus vector using the Gateway technique pAd/CMV/V5-DEST™ (Invitrogen, Carlsbad, CA, USA) as described by the manufacturer. Adenoviral vectors were then linearised with PacI before they were transfected to HEK293A cells. The virus was harvested and further amplified by reinfecting HEK293A cells. The adenovirus was eventually purified using the Adeno-X™ Maxi Purification Kit (Clontech, Mountain View, CA, USA) according to the manufacturer's instructions. Infectious units of both lenti- and adeno-miRNA viruses were determined by titration in HEK293T cells.

4.8 | IAV infection

HEK293 cells were seeded in a 12-well plate (5×10^5 cells per well) and then transfected with 1.25 μg of pENTR-miRNA or miR-Con vector using Lipofectamine 3000 (Thermo Fisher Scientific, Waltham, MA, USA) for 24 hr. A549 cells were seeded in a 12-well plate (2×10^5 cells per well) and then infected with miR-193b or miR-Con lentivirus at a MOI of 100 for 48 hr. Thereafter, the cells were infected with IAV at the indicated MOIs in serum-free medium containing 0.5 μg/ml of trypsin treated with L-(tosylamido-2-phenyl) ethyl chloromethyl ketone (TPCK; Worthington Biochemical Corporation, Lakewood, NJ, USA). At 1-hr postviral absorption, the inoculum was removed, and serum-free medium containing 0.3% bovine serum albumin (BSA, Sigma, St. Louis, MO, USA) and 0.5 μg/ml of TPCK-treated trypsin was added and incubated for the indicated times. The cells were collected for mRNA and protein analyses, and the culture media were collected for titre determination.

4.9 | Median tissue culture infective dose (TCID$_{50}$) assay

Virus titrations were performed according to a protocol adapted from De Vleeschauwer, Van Poucke, Karasin, Olsen, and Van Reeth (2011). Briefly, MDCK cells were seeded in a 96-well cell culture plate at a density of 20,000 cells per well. One day after seeding, the cells were inoculated with 50 μl of 10-fold serially diluted samples. After 1 hr, the inoculum was removed, followed by the addition of serum-free DMEM containing 1-μg/ml TPCK-trypsin. The cells were observed daily for 5 days for the appearance of cytopathic effects. Virus titres were calculated according to the method of Reed and Muench (Reed & Hugo, 1938).

4.10 | Reverse transcription and real-time PCR

To measure mRNA expression levels, total RNA was extracted using TRI Reagent® (Molecular Research Center, Cincinnati, OH, USA). One microgram of RNA was treated with RNase-Free DNase I (Thermo Scientific, Waltham, MA, USA) at 37°C for 30 min and then reverse-transcribed using M-MLV Reverse Transcriptase (Thermo Fisher Scientific, Waltham, MA, USA) with oligo (dT)18 and random hexamer primers (Promega, Madison, WI, USA). Real-time PCR was carried out in a 20-μl reaction volume containing specific primers (Table 1) and SYBR Green PCR Master Mix (Eurogentec, Fremont, CA, USA). PCR was performed on an ABI 7500 real-time PCR System (Applied Biosystems, Foster City, CA, USA). The cycling conditions for real-time PCR were as follows: 95°C for 1 min, followed by 40 cycles of 95°C for 15 s and 60°C for 1 min. The expression level of a gene was normalised to the internal control, β-actin, and the expression level was calculated using the $2^{-\Delta Ct}$ method.

4.11 | Real-time PCR for miRNA expression

Total RNA was extracted using TRI Reagent® and then polyadenylated using the Poly(A) Polymerase Tailing Kit (NEB, MA,

TABLE 1 Real-time PCR primers

Primer name	Forward primers 5'-3'	Reverse primers 5'-3'
hsa-miR-193b	AACTGGCCCTCAAAGTCCCG	GCGAGCACAGAATTAATACGAC
hsa-miR-548f-1	TGCAAAAGTAATCACAGTT	GCGAGCACAGAATTAATACGAC
hsa-miR-1-1	TGGAATGTAAAGAAGTATGTAT	GCGAGCACAGAATTAATACGAC
Has-miR-509-1	TGATTGGTACGTCTGTGGGTAG	GCGAGCACAGAATTAATACGAC
PolyT adapter	GCGAGCACAGAATTAATACGACTCACTATAGGTTTTTTTTTTTTTTVN (N = A + C + G + T, V = G + A + C)	
NP	TGTGTATGGACCTGCCGTAGC	CCATCCACACCAGTTGACTCTTG
NS1	TGGAAAGCAAATAGTGGAGCG	GTAGCGCGATGCAGGTACAGAG
PB1	CCGATGCCATAGAGGTGACA	GGAGACCAGCAGTCCAGCTTT
LEF1	GCTTTATCCAGGCTGGTCTGCAA	GACCTGTACCTGATGCAGATTCCT
CTNNB1	CATCTACACAGTTTGATGCTGCT	GCAGTTTTGTCAGTTCAGGGA
FZD4	TTTCACACCGCTCATCCAGTAC	GGGTTCACAGCTCTCTTGACT
CCND1	GCAGACCTTCGTTGCCCTCT	GCGTGTGAGGCGGTAAGTAGG
c-myc	TGGTCGCCCTCCTATGTTG	CCGGGTCGCAGATGAAACTC

USA). Briefly, a 10-µl reaction containing 1 µg total RNA, 1 µl of 10 × reaction buffer, 1 µl of 10 mM ATP and 5 units of *Escherichia coli* Poly(A) Polymerase was incubated at 37°C for 20 min, followed by enzyme inactivation at 65°C for 20 min. After polyadenylation, reverse transcription was performed using 10 µl of the polyadenylated reaction product, 1 µl of 0.5 µM Poly(T) adapter, 1 µl of 10 mM dNTP, and 1 µl of M-MLV Reverse Transcriptase. The reaction was incubated at 37°C for 50 min and then terminated by heating at 70°C for 15 min. Real-time PCR were performed using SYBR green PCR master mix with the above-described conditions. The expression of a miRNA was analysed according to the comparative Ct method by normalisation to U48 or U6 small nuclear RNA using the $2^{-\Delta Ct}$ method.

4.12 | Luciferase reporter assay

For the 3′-UTR reporter assay, HEK293T cells were transfected with 5 ng of 3′-UTR reporter vector, 100 ng of miRNA or miR-con vector using Lipofectamine 2000. Two days after transfection, the cells were harvested for the dual luciferase activity assay.

To determine the effect of miR-193b on different strains of IAV replication, a viral luciferase reporter assay was performed. Briefly, HEK293 or A549 cells were transfected with an IAV reporter vector pHH21-NP-3′-UTR-LUC-NP-5′-UTR (20 ng), a miR-193b pENTR or miR-con vector (100 ng), and a normalisation pRL-TK vector (2 ng) using Lipofectamine 3000. Twenty-four hours post transfection, the cells were infected with different strains of IAV, A/PR/8/34 (MOI 0.01), OK/09 (MOI 0.01), A/WSN/33 (MOI 0.005), or A/Oklahoma/ 309/2006 (MOI 0.01) for 48 hr. The cells were lysed, and the dual luciferase assay was performed. The reporter activity was expressed as a ratio of firefly to *Renilla* activities, which was further normalised to miR-con.

4.13 | Western blot analysis

The cells were lysed with an appropriate volume of protein lysis buffer (Thermo Fisher Scientific, Waltham, MA, USA) containing phosphatase and protease inhibitors (Thermo Fisher Scientific, Waltham, MA, USA). The protein concentration was then determined using the Bio-Rad Protein Assay Kit (Bio-Rad, CA, USA). Ten micrograms of each protein sample were electrophoresed by SDS-PAGE and transferred onto a nitrocellulose membrane. Western blot analysis was performed using the following primary antibodies and dilutions: mouse anti-NP (ATCC, HB-65, 1:50), mouse anti-NS1 (Santa Cruz biotechnology, Santa Cruz, CA, USA, 1:1000), mouse anti-β-actin (Thermo Fisher Scientific, 1:3000), rabbit anti-β-catenin (Cell Signaling, Beverly, MA, USA, 1:1000), rabbit anti-LEF1 (Cell Signaling, 1:1000), and rabbit anti-FZD4 (Cell Signaling, 1:1000). The membranes were incubated with primary antibodies overnight at 4°C, followed by incubation with horseradish peroxidase (HRP)-conjugated goat anti-mouse IgG (Jackson ImmunoResearch, PA, USA, 1:2000) or goat anti-rabbit IgG (Jackson ImmunoResearch, 1:2000) at room temperature for 1 hr. Protein bands were visualised using the enhanced chemiluminescence kit (Thermo Fisher Scientific, Rockford, IL, USA).

4.14 | IF staining

For viral NP IF staining, lenti-miR-193b or vector control-infected A549 cells were seeded in a 96-well plate and then infected with A/PR/8/34 virus at an MOI of 10. The cells were then fixed for 20 min in 4% paraformaldehyde and permeabilised for 20 min with 0.2% Triton X-100. Next, the cells were incubated with mouse anti-NP primary IgG antibodies (ATCC, HB-65, 1:20) in PBS containing 10% normal goat serum for 1 hr at 37°C, followed by Alexa Flour 546-conjugated goat anti-mouse IgG secondary antibodies (Life Technologies, Carlsbad, CA, 1:300) in PBS containing 10% normal goat serum for 1 hr at 37°C. Cell nuclei were stained with 2 µg/ml of Hoechst 33342 dye (Molecular Probes, Waltham, MA). The fluorescence signal was examined with a Nikon fluorescence microscope. The total number of NP nuclear-centred cells and the total number of cells were counted. Data were then presented as percentages of NP nuclear-localised cells over total cells in miR-193b-infected cells versus miR-Con infected cells.

4.15 | sgRNA design and generation of the miR-193b knockout cell lines

Two single guide RNAs (sgRNAs) were designed by using online software (http://chopchop.cbu.uib.no/). The PAM sequence near the miR-193b seed sequence and the 20-bp sequence upstream were chosen. We constructed the lentiviral CRISPR/Cas9 mediated miR-193b gene editing vectors by subcloning each annealed sgRNA oligonucleotide pair into the sgRNA scaffold of lentiCRISPR v2 vector (Addgene, #52961) via the BsmII sites. A control vector was constructed by inserting an EGFP sgRNA sequence into the same vector. Lentivirus was prepared by transfecting sgRNA-lentiCRISPR v2 vector and package plasmids pSPAX2 and pMD2G into HEK293T cells using PEI reagent. Stable cell lines were generated by infecting A549 cells with the CRISPR/Cas9 lentivirus containing sgRNA and selected with 1-µg/ml puromycin.

To detect Indels, genomic DNA was isolated from the CRISPR/Cas9-edited cells, and the targeted locus that encompasses the mature miR-193b region was PCR-amplified using the following primers: Forward 5′AGCTTTGGTCATCAAAATAGGA3′, Reverse 5′ ATTGGAGTTTATCGGCAACTGT3′. The PCR products were denatured, annealed and digested with T7 endonuclease I (NEB, Ipswich, MA, USA), which recognises and cleaves nonperfectly matched DNA, at 37°C for 60 min. Digested products were separated on a 1% agarose gel for imaging and cloned into the pGEM-T vector (Promega, Madison, WI, USA) for DNA sequencing.

4.16 | Cell cycle analysis

A549 cells were infected with a miR-193b lentivirus or control virus (MOI 100) for 48 hr. The cells were trypsinised and then seeded in a 12-well plate (10^5 cells per well). At 12 hr after seeding, the medium was replaced with serum free F-12K and cultured for 48 hr. The medium was then replaced with F-12K containing 10% FBS and cultured for 18 and 30 hr. The cells were trypsinised and fixed with

ethanol at −20°C for at least 2 hr. At the time of analysis, the cells were centrifuged and stained with a freshly made solution containing propidium iodide provided with the cell cycle phase determination kit (Cayman, Ann Arbor, MI, USA), according to the manufacturer's instructions. The cell cycle distribution was measured using a flow cytometer (Accuri C6, BD Biosciences) and analysed with BD Sampler Software.

4.17 | Animal studies

The animal procedures were approved by the Institutional Animal Care and Use Committee at Oklahoma State University. miR-193b adenovirus or control virus (10^9 IFU) in 50 μl of PBS were delivered via intratracheal inoculation to the lungs of 8-week-old female C57BL/6J mice 2 days before IAV challenge. IAV infection was performed by intranasal inoculation of 250 PFU of A/PR/8/34 in 50 μl of PBS. Body weight loss was monitored daily. Mice were euthanised at Day 3 or 7 post infection. The left lungs of mice were fixed in 10% neutral-buffered formalin (Thermo Scientific, West Palm Beach, FL, USA). The right lungs were snap-frozen in liquid nitrogen and powered under liquid nitrogen using a mortar and pestle. The powder was divided into three parts: one dissolved in TRI Reagent® for RNA isolation, one in protein lysis buffer for western blot analysis, and one in DMEM (100 mg/ml) for determination of the viral titre.

CONFLICT OF INTEREST

The authors have no conflict of interest to declare.

ORCID

Lin Liu https://orcid.org/0000-0002-4811-4897

REFERENCES

Ahrens, M. J., Romereim, S., & Dudley, A. T. (2011). A re-evaluation of two key reagents for in vivo studies of Wnt signaling. *Developmental Dynamics*, 240(9), 2060–2068. https://doi.org/10.1002/dvdy.22704

Akhtar, M. M., Micolucci, L., Islam, M. S., Olivieri, F., & Procopio, A. D. (2016). Bioinformatic tools for microRNA dissection. *Nucleic Acids Research*, 44(1), 24–44. https://doi.org/10.1093/nar/gkv1221

Anton, R., Chatterjee, S. S., Simundza, J., Cowin, P., & Dasgupta, R. (2011). A systematic screen for micro-RNAs regulating the canonical Wnt pathway. *PLoS One*, 6(10), e26257. https://doi.org/10.1371/journal.pone.0026257

Bagga, S., & Bouchard, M. J. (2014). Cell cycle regulation during viral infection. *Methods in Molecular Biology*, 1170, 165–227. https://doi.org/10.1007/978-1-4939-0888-2_10

Baldin, V., Lukas, J., Marcote, M. J., Pagano, M., & Draetta, G. (1993). Cyclin D1 is a nuclear protein required for cell cycle progression in G1. *Genes & Development*, 7(5), 812–821. https://doi.org/10.1101/gad.7.5.812

Baril, M., Es-Saad, S., Chatel-Chaix, L., Fink, K., Pham, T., Raymond, V. A., ... Lamarre, D. (2013). Genome-wide RNAi screen reveals a new role of a WNT/CTNNB1 signaling pathway as negative regulator of virus-induced innate immune responses. *PLoS Pathogens*, 9(6), e1003416. https://doi.org/10.1371/journal.ppat.1003416

Barr, I. G., Hurt, A. C., Deed, N., Iannello, P., Tomasov, C., & Komadina, N. (2007). The emergence of adamantane resistance in influenza A(H1) viruses in Australia and regionally in 2006. *Antiviral Research*, 75(2), 173–176. https://doi.org/10.1016/j.antiviral.2007.01.006

Barrett, S., & McKimm-Breschkin, J. L. (2014). Solid phase assay for comparing reactivation rates of neuraminidases of influenza wild type and resistant mutants after inhibitor removal. *Antiviral Research*, 108, 30–35. https://doi.org/10.1016/j.antiviral.2014.05.006

Barth, A. I., Stewart, D. B., & Nelson, W. J. (1999). T cell factor-activated transcription is not sufficient to induce anchorage-independent growth of epithelial cells expressing mutant β-catenin. *Proceedings of the National Academy of Sciences of the United States of America*, 96(9), 4947–4952. https://doi.org/10.1073/pnas.96.9.4947

Bhaskaran, M., Wang, Y., Zhang, H., Weng, T., Baviskar, P., Guo, Y., ... Liu, L. (2009). MicroRNA-127 modulates fetal lung development. *Physiological Genomics*, 37(3), 268–278. https://doi.org/10.1152/physiolgenomics.90268.2008

Bright, R. A., Medina, M. J., Xu, X., Perez-Oronoz, G., Wallis, T. R., Davis, X. M., ... Klimov, A. I. (2005). Incidence of adamantane resistance among influenza A (H3N2) viruses isolated worldwide from 1994 to 2005: A cause for concern. *Lancet*, 366(9492), 1175–1181. https://doi.org/10.1016/S0140-6736(05)67338-2

Cavallo, R. A., Cox, R. T., Moline, M. M., Roose, J., Polevoy, G. A., Clevers, H., ... Bejsovec, A. (1998). *Drosophila* Tcf and Groucho interact to repress Wingless signalling activity. *Nature*, 395(6702), 604–608. https://doi.org/10.1038/26982

Cawood, R., Harrison, S. M., Dove, B. K., Reed, M. L., & Hiscox, J. A. (2007). Cell cycle dependent nucleolar localization of the coronavirus nucleocapsid protein. *Cell Cycle*, 6(7), 863–867. https://doi.org/10.4161/cc.6.7.4032

Chang, H., Yi, B., Ma, R., Zhang, X., Zhao, H., & Xi, Y. (2016). CRISPR/cas9, a novel genomic tool to knock down microRNA in vitro and in vivo. *Scientific Reports*, 6, 22312. https://doi.org/10.1038/srep22312

Chen, J., Feilotter, H. E., Pare, G. C., Zhang, X., Pemberton, J. G., Garady, C., ... Tron, V. A. (2010). MicroRNA-193b represses cell proliferation and regulates cyclin D1 in melanoma. *The American Journal of Pathology*, 176(5), 2520–2529. https://doi.org/10.2353/ajpath.2010.091061

Davidson, G., & Niehrs, C. (2010). Emerging links between CDK cell cycle regulators and Wnt signaling. *Trends in Cell Biology*, 20(8), 453–460. https://doi.org/10.1016/j.tcb.2010.05.002

de Lau, W., & Clevers, H. (2001). LEF1 turns over a new leaf. *Nature Genetics*, 28(1), 3–4. https://doi.org/10.1038/88233

De Vleeschauwer, A. R., Van Poucke, S. G., Karasin, A. I., Olsen, C. W., & Van Reeth, K. (2011). Cross-protection between antigenically distinct H1N1 swine influenza viruses from Europe and North America. *Influenza and Other Respiratory Viruses*, 5(2), 115–122. https://doi.org/10.1111/j.1750-2659.2010.00164.x

Emmett, S. R., Dove, B., Mahoney, L., Wurm, T., & Hiscox, J. A. (2005). The cell cycle and virus infection. *Methods in Molecular Biology*, 296, 197–218.

Gao, X. N., Lin, J., Gao, L., Li, Y. H., Wang, L. L., & Yu, L. (2011). MicroRNA-193b regulates c-Kit proto-oncogene and represses cell proliferation in acute myeloid leukemia. *Leukemia Research*, 35(9), 1226–1232. https://doi.org/10.1016/j.leukres.2011.06.010

Gaur, P., Munjhal, A., & Lal, S. K. (2011). Influenza virus and cell signaling pathways. *Medical Science Monitor*, 17(6), RA148–RA154.

Guo, Y., Mishra, A., Weng, T., Chintagari, N. R., Wang, Y., Zhao, C., ... Liu, L. (2014). Wnt3a mitigates acute lung injury by reducing P2X7 receptor-mediated alveolar epithelial type I cell death. *Cell Death & Disease*, 5, e1286. https://doi.org/10.1038/cddis.2014.254

Harmon, B., Bird, S. W., Schudel, B. R., Hatch, A. V., Rasley, A., & Negrete, O. A. (2016). A genome-wide RNA interference screen identifies a role for Wnt/beta-catenin signaling during Rift Valley fever virus infection. *Journal of Virology*, 90(16), 7084–7097. https://doi.org/10.1128/JVI.00543-16

He, Y., Xu, K., Keiner, B., Zhou, J., Czudai, V., Li, T., ... Sun, B. (2010). Influenza A virus replication induces cell cycle arrest in G0/G1 phase. *Journal of Virology*, 84(24), 12832–12840. https://doi.org/10.1128/JVI.01216-10

Hillesheim, A., Nordhoff, C., Boergeling, Y., Ludwig, S., & Wixler, V. (2014). β-catenin promotes the type I IFN synthesis and the IFN-dependent signaling response but is suppressed by influenza A virus-induced RIG-I/NF-κB signaling. *Cell Communication and Signaling: CCS*, 12, 29. https://doi.org/10.1186/1478-811X-12-29

Houser, K., & Subbarao, K. (2015). Influenza vaccines: Challenges and solutions. *Cell Host & Microbe*, 17(3), 295–300. https://doi.org/10.1016/j.chom.2015.02.012

Hu, H., Li, S., Liu, J., & Ni, B. (2012). MicroRNA-193b modulates proliferation, migration, and invasion of non-small cell lung cancer cells. *Acta Biochim Biophys Sin (Shanghai)*, 44(5), 424–430. https://doi.org/10.1093/abbs/gms018

Hu, T., Phiwpan, K., Guo, J., Zhang, W., Guo, J., Zhang, Z., ... Zhou, X. (2016). MicroRNA-142-3p negatively regulates canonical Wnt signaling pathway. *PLoS One*, 11(6), e0158432. https://doi.org/10.1371/journal.pone.0158432

Huang, C., Xiao, X., Yang, Y., Mishra, A., Liang, Y., Zeng, X., ... Liu, L. (2017). MicroRNA-101 attenuates pulmonary fibrosis by inhibiting fibroblast proliferation and activation. *The Journal of Biological Chemistry*, 292(40), 16420–16439. https://doi.org/10.1074/jbc.M117.805747

Huang, H. C., & Klein, P. S. (2004). The Frizzled family: Receptors for multiple signal transduction pathways. *Genome Biology*, 5(7), 234. https://doi.org/10.1186/gb-2004-5-7-234

Huang, K., Zhang, J. X., Han, L., You, Y. P., Jiang, T., Pu, P. Y., & Kang, C. S. (2010). MicroRNA roles in beta-catenin pathway. *Molecular Cancer*, 9, 252. https://doi.org/10.1186/1476-4598-9-252

Hudson, R. S., Yi, M., Esposito, D., Watkins, S. K., Hurwitz, A. A., Yfantis, H. G., ... Ambs, S. (2012). MicroRNA-1 is a candidate tumor suppressor and prognostic marker in human prostate cancer. *Nucleic Acids Research*, 40(8), 3689–3703. https://doi.org/10.1093/nar/gkr1222

Hurt, A. C., Ernest, J., Deng, Y. M., Iannello, P., Besselaar, T. G., Birch, C., ... Barr, I. G. (2009). Emergence and spread of oseltamivir-resistant A(H1N1) influenza viruses in Oceania, South East Asia and South Africa. *Antiviral Research*, 83(1), 90–93. https://doi.org/10.1016/j.antiviral.2009.03.003

Ishitani, T., Matsumoto, K., Chitnis, A. B., & Itoh, M. (2005). Nrarp functions to modulate neural-crest-cell differentiation by regulating LEF1 protein stability. *Nature Cell Biology*, 7(11), 1106–1112. https://doi.org/10.1038/ncb1311

Jiang, W., Wang, Q., Chen, S., Gao, S., Song, L., Liu, P., & Huang, W. (2013). Influenza A virus NS1 induces G0/G1 cell cycle arrest by inhibiting the expression and activity of RhoA protein. *Journal of Virology*, 87(6), 3039–3052. https://doi.org/10.1128/JVI.03176-12

Jin, X., Sun, Y., Yang, H., Li, J., Yu, S., Chang, X., ... Chen, J. (2015). Deregulation of the MiR-193b-KRAS axis contributes to impaired cell growth in pancreatic cancer. *PLoS One*, 10(4), e0125515. https://doi.org/10.1371/journal.pone.0125515

Kamali, A., & Holodniy, M. (2013). Influenza treatment and prophylaxis with neuraminidase inhibitors: A review. *Infection and Drug Resistance*, 6, 187–198. https://doi.org/10.2147/IDR.S36601

Kojima, S., Chiyomaru, T., Kawakami, K., Yoshino, H., Enokida, H., Nohata, N., ... Seki, N. (2012). Tumour suppressors miR-1 and miR-133a target the oncogenic function of purine nucleoside phosphorylase (PNP) in prostate cancer. *British Journal of Cancer*, 106(2), 405–413. https://doi.org/10.1038/bjc.2011.462

Komiya, Y., & Habas, R. (2008). Wnt signal transduction pathways. *Organogenesis*, 4(2), 68–75. https://doi.org/10.4161/org.4.2.5851

Leivonen, S. K., Makela, R., Ostling, P., Kohonen, P., Haapa-Paananen, S., Kleivi, K., ... Kallioniemi, O. (2009). Protein lysate microarray analysis to identify microRNAs regulating estrogen receptor signaling in breast cancer cell lines. *Oncogene*, 28(44), 3926–3936. https://doi.org/10.1038/onc.2009.241

Li, G., Wang, Y., Liu, Y., Su, Z., Liu, C., Ren, S., ... Qiu, Y. (2014). miR-185-3p regulates nasopharyngeal carcinoma radioresistance by targeting WNT2B in vitro. *Cancer Science*, 105(12), 1560–1568. https://doi.org/10.1111/cas.12555

Li, X. F., Yan, P. J., & Shao, Z. M. (2009). Downregulation of miR-193b contributes to enhance urokinase-type plasminogen activator (uPA) expression and tumor progression and invasion in human breast cancer. *Oncogene*, 28(44), 3937–3948. https://doi.org/10.1038/onc.2009.245

Liu, B., Qu, J., Xu, F., Guo, Y., Wang, Y., Yu, H., & Qian, B. (2015). MiR-195 suppresses non-small cell lung cancer by targeting CHEK1. *Oncotarget*, 6(11), 9445–9456. https://doi.org/10.18632/oncotarget.3255

Liu, J., Ruan, B., You, N., Huang, Q., Liu, W., Dang, Z., ... Dou, K. (2013). Downregulation of miR-200a induces EMT phenotypes and CSC-like signatures through targeting the β-catenin pathway in hepatic oval cells. *PLoS One*, 8(11), e79409. https://doi.org/10.1371/journal.pone.0079409

Liu, X., Zhao, Z., Xu, C., Sun, L., Chen, J., Zhang, L., & Liu, W. (2012). Cyclophilin A restricts influenza A virus replication through degradation of the M1 protein. *PLoS One*, 7(2), e31063. https://doi.org/10.1371/journal.pone.0031063

Ludwig, S., & Planz, O. (2008). Influenza viruses and the NF-κB signaling pathway—Towards a novel concept of antiviral therapy. *Biological Chemistry*, 389(10), 1307–1312. https://doi.org/10.1515/BC.2008.148

Lutz, A., Dyall, J., Olivo, P. D., & Pekosz, A. (2005). Virus-inducible reporter genes as a tool for detecting and quantifying influenza A virus replication. *Journal of Virological Methods*, 126(1–2), 13–20. https://doi.org/10.1016/j.jviromet.2005.01.016

Ma, N., Zhang, W., Qiao, C., Luo, H., Zhang, X., Liu, D., ... Bai, J. (2016). The tumor suppressive role of MiRNA-509-5p by targeting FOXM1 in non-small cell lung cancer. *Cellular Physiology and Biochemistry*, 38(4), 1435–1446. https://doi.org/10.1159/000443086

Mao, K., Zhang, J., He, C., Xu, K., Liu, J., Sun, J., ... Xiao, Z. (2014). Restoration of miR-193b sensitizes hepatitis B virus-associated hepatocellular carcinoma to sorafenib. *Cancer Letters*, 352(2), 245–252. https://doi.org/10.1016/j.canlet.2014.07.004

Masamha, C. P., & Benbrook, D. M. (2009). Cyclin D1 degradation is sufficient to induce G1 cell cycle arrest despite constitutive expression of cyclin E2 in ovarian cancer cells. *Cancer Research*, 69(16), 6565–6572. https://doi.org/10.1158/0008-5472.CAN-09-0913

More, S., Yang, X., Zhu, Z., Bamunuarachchi, G., Guo, Y., Huang, C., ... Liu, L. (2018). Regulation of influenza virus replication by Wnt/β-catenin signaling. *PLoS One*, 13(1), e0191010. https://doi.org/10.1371/journal.pone.0191010

Nailwal, H., Sharma, S., Mayank, A. K., & Lal, S. K. (2015). The nucleoprotein of influenza A virus induces p53 signaling and apoptosis via attenuation of host ubiquitin ligase RNF43. *Cell Death & Disease*, 6, e1768. https://doi.org/10.1038/cddis.2015.131

Nasser, M. W., Datta, J., Nuovo, G., Kutay, H., Motiwala, T., Majumder, S., ... Ghoshal, K. (2008). Down-regulation of micro-RNA-1 (miR-1) in lung

cancer. Suppression of tumorigenic property of lung cancer cells and their sensitization to doxorubicin-induced apoptosis by miR-1. *Journal of Biological Chemistry*, *283*(48), 33394–33405. https://doi.org/10.1074/jbc.M804788200

Niehrs, C., & Acebron, S. P. (2012). Mitotic and mitogenic Wnt signalling. *The EMBO Journal*, *31*(12), 2705–2713. https://doi.org/10.1038/emboj.2012.124

Olmeda, D., Castel, S., Vilaro, S., & Cano, A. (2003). β-Catenin regulation during the cell cycle: Implications in G2/M and apoptosis. *Molecular Biology of the Cell*, *14*(7), 2844–2860. https://doi.org/10.1091/mbc.E03-01-0865

Orozovic, G., Orozovic, K., Jarhult, J. D., & Olsen, B. (2014). Study of oseltamivir and zanamivir resistance-related mutations in influenza viruses isolated from wild mallards in Sweden. *PLoS One*, *9*(2), e89306. https://doi.org/10.1371/journal.pone.0089306

Otsuka, M., Jing, Q., Georgel, P., New, L., Chen, J., Mols, J., ... Han, J. (2007). Hypersusceptibility to vesicular stomatitis virus infection in Dicer1-deficient mice is due to impaired miR24 and miR93 expression. *Immunity*, *27*(1), 123–134. https://doi.org/10.1016/j.immuni.2007.05.014

Radu, A., Neubauer, V., Akagi, T., Hanafusa, H., & Georgescu, M. M. (2003). PTEN induces cell cycle arrest by decreasing the level and nuclear localization of cyclin D1. *Molecular and Cellular Biology*, *23*(17), 6139–6149. https://doi.org/10.1128/MCB.23.17.6139-6149.2003

Rauhala, H. E., Jalava, S. E., Isotalo, J., Bracken, H., Lehmusvaara, S., Tammela, T. L., ... Visakorpi, T. (2010). miR-193b is an epigenetically regulated putative tumor suppressor in prostate cancer. *International Journal of Cancer*, *127*(6), 1363–1372. https://doi.org/10.1002/ijc.25162

Reed, L. J., & Hugo, M. (1938). A simple method of estimating fifty per cent endpoints. *Am J Hygiene*, *27*(3), 493–497.

Shapira, S. D., Gat-Viks, I., Shum, B. O., Dricot, A., de Grace, M. M., Wu, L., ... Hacohen, N. (2009). A physical and regulatory map of host-influenza interactions reveals pathways in H1N1 infection. *Cell*, *139*(7), 1255–1267. https://doi.org/10.1016/j.cell.2009.12.018

Shiah, S. G., Hsiao, J. R., Chang, W. M., Chen, Y. W., Jin, Y. T., Wong, T. Y., ... Chang, J. Y. (2014). Downregulated miR329 and miR410 promote the proliferation and invasion of oral squamous cell carcinoma by targeting Wnt-7b. *Cancer Research*, *74*(24), 7560–7572. https://doi.org/10.1158/0008-5472.CAN-14-0978

Shtutman, M., Zhurinsky, J., Simcha, I., Albanese, C., D'Amico, M., Pestell, R., & Ben-Ze'ev, A. (1999). The cyclin D1 gene is a target of the β-catenin/LEF-1 pathway. *Proceedings of the National Academy of Sciences of the United States of America*, *96*(10), 5522–5527. https://doi.org/10.1073/pnas.96.10.5522

Smith, J. L., Jeng, S., McWeeney, S. K., & Hirsch, A. J. (2017). A microRNA screen identifies the Wnt signaling pathway as a regulator of the interferon response during flavivirus infection. *Journal of Virology*, *91*(8). https://doi.org/10.1128/JVI.02388-16

Soema, P. C., Kompier, R., Amorij, J. P., & Kersten, G. F. (2015). Current and next generation influenza vaccines: Formulation and production strategies. *European Journal of Pharmaceutics and Biopharmaceutics*, *94*, 251–263. https://doi.org/10.1016/j.ejpb.2015.05.023

Song, L., Liu, H., Gao, S., Jiang, W., & Huang, W. (2010). Cellular microRNAs inhibit replication of the H1N1 influenza A virus in infected cells. *Journal of Virology*, *84*(17), 8849–8860. https://doi.org/10.1128/JVI.00456-10

Tang, H., Kong, Y., Guo, J., Tang, Y., Xie, X., Yang, L., ... Xie, X. (2013). Diallyl disulfide suppresses proliferation and induces apoptosis in human gastric cancer through Wnt-1 signaling pathway by up-regulation of miR-200b and miR-22. *Cancer Letters*, *340*(1), 72–81. https://doi.org/10.1016/j.canlet.2013.06.027

Thibault, P. A., Huys, A., Amador-Canizares, Y., Gailius, J. E., Pinel, D. E., & Wilson, J. A. (2015). Regulation of hepatitis C virus genome replication by Xrn1 and microRNA-122 binding to individual sites in the 5′ untranslated region. *Journal of Virology*, *89*(12), 6294–6311. https://doi.org/10.1128/JVI.03631-14

Tian, Y., Pan, Q., Shang, Y., Zhu, R., Ye, J., Liu, Y., ... Wang, R. (2014). MicroRNA-200 (miR-200) cluster regulation by achaete scute-like 2 (Ascl2): Impact on the epithelial-mesenchymal transition in colon cancer cells. *The Journal of Biological Chemistry*, *289*(52), 36101–36115. https://doi.org/10.1074/jbc.M114.598383

Turpin, E., Luke, K., Jones, J., Tumpey, T., Konan, K., & Schultz-Cherry, S. (2005). Influenza virus infection increases p53 activity: Role of p53 in cell death and viral replication. *Journal of Virology*, *79*(14), 8802–8811. https://doi.org/10.1128/JVI.79.14.8802-8811.2005

Vleminckx, K., Kemler, R., & Hecht, A. (1999). The C-terminal transactivation domain of β-catenin is necessary and sufficient for signaling by the LEF-1/β-catenin complex in *Xenopus laevis*. *Mechanisms of Development*, *81*(1–2), 65–74. https://doi.org/10.1016/S0925-4773(98)00225-1

Wang, P., Hou, J., Lin, L., Wang, C., Liu, X., Li, D., ... Cao, X. (2010). Inducible microRNA-155 feedback promotes type I IFN signaling in antiviral innate immunity by targeting suppressor of cytokine signaling 1. *Journal of Immunology*, *185*(10), 6226–6233. https://doi.org/10.4049/jimmunol.1000491

Wang, Y., Stricker, H. M., Gou, D., & Liu, L. (2007). MicroRNA: Past and present. *Frontiers in Bioscience*, *12*, 2316–2329. https://doi.org/10.2741/2234

Wang, Z., Humphries, B., Xiao, H., Jiang, Y., & Yang, C. (2014). MicroRNA-200b suppresses arsenic-transformed cell migration by targeting protein kinase Cα and Wnt5b-protein kinase Cα positive feedback loop and inhibiting Rac1 activation. *The Journal of Biological Chemistry*, *289*(26), 18373–18386. https://doi.org/10.1074/jbc.M114.554246

Watanabe, T., Kawakami, E., Shoemaker, J. E., Lopes, T. J., Matsuoka, Y., Tomita, Y., ... Kawaoka, Y. (2014). Influenza virus-host interactome screen as a platform for antiviral drug development. *Cell Host & Microbe*, *16*(6), 795–805. https://doi.org/10.1016/j.chom.2014.11.002

Watanabe, T., Watanabe, S., & Kawaoka, Y. (2010). Cellular networks involved in the influenza virus life cycle. *Cell Host & Microbe*, *7*(6), 427–439. https://doi.org/10.1016/j.chom.2010.05.008

Wu, W., Lin, Z., Zhuang, Z., & Liang, X. (2009). Expression profile of mammalian microRNAs in endometrioid adenocarcinoma. *European Journal of Cancer Prevention*, *18*(1), 50–55. https://doi.org/10.1097/CEJ.0b013e328305a07a

Wurzer, W. J., Planz, O., Ehrhardt, C., Giner, M., Silberzahn, T., Pleschka, S., & Ludwig, S. (2003). Caspase 3 activation is essential for efficient influenza virus propagation. *The EMBO Journal*, *22*(11), 2717–2728. https://doi.org/10.1093/emboj/cdg279

Xu, C., Liu, S., Fu, H., Li, S., Tie, Y., Zhu, J., ... Zheng, X. (2010). MicroRNA-193b regulates proliferation, migration and invasion in human hepatocellular carcinoma cells. *European Journal of Cancer*, *46*(15), 2828–2836. https://doi.org/10.1016/j.ejca.2010.06.127

York, A., Hutchinson, E. C., & Fodor, E. (2014). Interactome analysis of the influenza A virus transcription/replication machinery identifies protein phosphatase 6 as a cellular factor required for efficient virus replication. *Journal of Virology*, *88*(22), 13284–13299. https://doi.org/10.1128/JVI.01813-14

Zamore, P. D., & Haley, B. (2005). Ribo-gnome: The big world of small RNAs. *Science*, *309*(5740), 1519–1524. https://doi.org/10.1126/science.1111444

Zhang, C., Wu, Y., Xuan, Z., Zhang, S., Wang, X., Hao, Y., ... Zhang, S. (2014). p38MAPK, Rho/ROCK and PKC pathways are involved in influenza-induced cytoskeletal rearrangement and hyperpermeability in PMVEC via phosphorylating ERM. *Virus Research*, *192*, 6–15. https://doi.org/10.1016/j.virusres.2014.07.027

Zhang, W. B., Pan, Z. Q., Yang, Q. S., & Zheng, X. M. (2013). Tumor suppressive miR-509-5p contributes to cell migration, proliferation and antiapoptosis in renal cell carcinoma. *Irish Journal of Medical Science*, *182*(4), 621–627. https://doi.org/10.1007/s11845-013-0941-y

Zhang, X., Li, M., Zuo, K., Li, D., Ye, M., Ding, L., ... Lv, Z. (2013). Upregulated miR-155 in papillary thyroid carcinoma promotes tumor growth by targeting APC and activating Wnt/β-catenin signaling. *The Journal of Clinical Endocrinology and Metabolism*, *98*(8), E1305–E1313. https://doi.org/10.1210/jc.2012-3602

Zhao, S., Ye, X., Xiao, L., Lian, X., Feng, Y., Li, F., & Li, L. (2014). MiR-26a inhibits prostate cancer progression by repression of Wnt5a. *Tumour Biology*, *35*(10), 9725–9733. https://doi.org/10.1007/s13277-014-2206-4

Zhirnov, O. P., & Klenk, H. D. (2007). Control of apoptosis in influenza virus-infected cells by up-regulation of Akt and p53 signaling. *Apoptosis*, *12*(8), 1419–1432. https://doi.org/10.1007/s10495-007-0071-y

SUPPORTING INFORMATION

Additional supporting information may be found online in the Supporting Information section at the end of the article.

How to cite this article: Yang X, Zhao C, Bamunuarachchi G, et al. miR-193b represses influenza A virus infection by inhibiting Wnt/β-catenin signalling. *Cellular Microbiology*. 2019;21:e13001. https://doi.org/10.1111/cmi.13001